A General concept

FORMIND 3.0 is an individual-based, spatially explicit and process-based model designed for simulating species-rich vegetation communities. This document introduces the full model description. The full model description of FORMIND 3.0 can also be found at www.formind.org. The description shows the entire range of different model versions, which can be currently applied (i.e. the choices of different geometries of the vegetation, of the climatic zone or of various disturbance events).

In FORMIND 3.0 vegetation is simulated on an area of size A_{area}, which is a composite of regularly ordered, quadratic patches of size A_{patch} [m^2] described by their location within the area (Fig. 1). Individual trees grow within the patches, but do not have spatially explicit positions within a patch (the gap model approach).

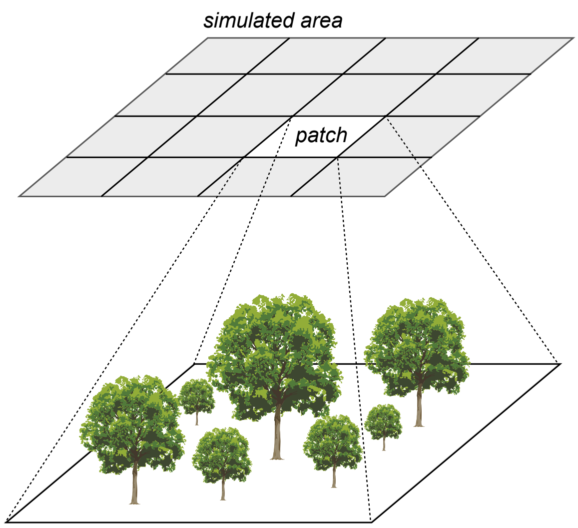

Figure 1: *Illustration of the simulated area and its composition of regularly ordered patches. Individual trees do not have spatially explicit positions within the patches. Only for an illustrative purpose, we show positioned trees on an exemplary patch.*

The trees change their size during the simulation according to a set of ecophysiological and morphological parameters used within the modelled processes. The modelled processes are simulated on different levels: (i) area-level, (ii) patch-level or (iii) on the level of a single tree .

- **Chapter B - Geometry**
  trees are described by several geometric relationships. tree types (in some projects

we use the concept of plant functional types in others real species) can differ in their parameter sets of these relationships.

Within each time step Δt (e.g. one year), the following main processes can be calculated:

- **Chapter C - Recruitment and establishment**
  Establishment of recruited seeds is modelled on the patch-level, whereby the distribution of seeds is simulated on the area-level.

- **Chapter D - Mortality**
  First, an event-driven mortality due to crowding can take place on the patch-level. Afterwards, mortality rates affects each trees (e.g. base mortality). Finally, every dying tree has a change to fall down and damage other trees .

- **Chapter E - Environment**
  The patches of the simulation area are homogeneously concerning climatic input variables. Based on these input parameters, the environment of the trees is specified. For example, the radiation above canopy and day length are equal for all patches. The vertical attenuation of the incoming radiation (i.e. light climate) is calculated for each patch based on the vegetation state, so that light intensity at different heights can differ between patches dependent on the number of trees shading each other. Reduced light availability result in a reduced gross photosynthesis of a tree . Limited soil water resources can also reduce the gross photosynthesis of an individual. In the same manner as the light climate, soil water contents can differ between patches during the simulation, although the initial soil water content and other soil properties (e.g. soil porosity) are equal for all patches. Differences in soil water content between patches are dependent on the number of trees per patch, which take up soil water resources. Further, type-specific effect of air temperature can also limit gross photosynthesis and affect respiration of an individual.

- **Chapter F - Growth**
  The growth of a single tree is determined by its gross productivity, respiration and type-specific morphological parameters. Respiration is calculated on the level of an individual. An increase in biomass per tree is modelled as the difference between gross photosynthesis and respiration. The allocation of the resulting biomass increase (including the increase of geometrical properties according to chapter B) act on the level of a tree .

- **Chapter G - Disturbances**
  Fire and landslide events are simulated on the area-level.

- **Chapter I - Logging**
  Selective logging of trees is simulated on the area-level. The selection is based on tree - specific characteristics (e.g. stem diameter or tree type) and represent conventional or reduced impact logging.

The modelled processes, which are summarized within the above mentioned main processes, are scheduled in a serial way. For an overview on the modelled processes and their schedule see Fig. 2.

Periodic or open boundary conditions can be used. For periodic boundary conditions, that means processes leaving one side of the simulation area are entering the area on the opposite side again. For open boundary conditions, that means processes leaving the simulation area are lost. No migration entering the open boundaries would be considered.

For the purpose of calculations within the processes of light climate and crowding mortality, the above-ground space is discretized into vertical height layers of constant width Δh. Table 1 shows general input parameters.

Table 1: *Parameters describing space and time.*

Description	Parameter	Unit	values range
Time step	Δt	year	$365^{-1} - 5$
Simulation area	A_{area}	hectare	1-400
Patch area	A_{patch}	m^2	400
Width of height layers	Δh	m	0.5

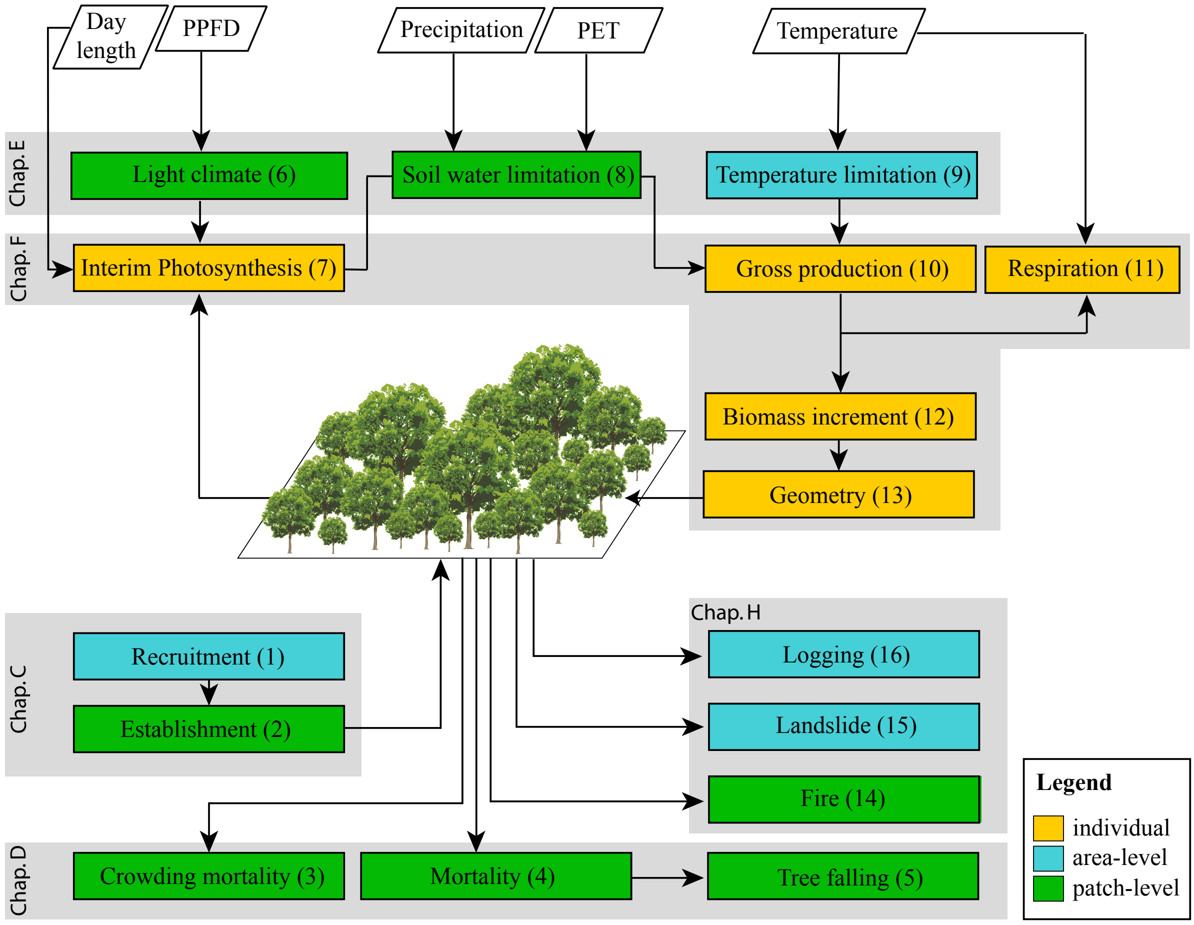

Figure 2: *Block diagram of the modelled processes. Different colours indicate the spatial scale on which each process is calculated (blue = area, green = patch, orange= individual). Italic written boxes show processes which are simulated with time steps of higher resolution than Δt (e.g one year). Numbers in brackets within each box show the serial order of their calculation within one time step Δt. Grey frames that underly these boxes group them according to the above mentioned main processes and their corresponding chapters. Rhombuses indicate climatic input parameters with the following abbreviations: PET – potential evapotranspiration, PPFD – photoactive photon flux density.*

B Geometry

Although individual trees in real forests do not necessarily have identical shapes, we model each tree by a cylindrical stem and a cylindrical crown (Fig. 3). The geometry of an individual can be described completely by the following size characteristics: stem diameter (D), height (H), crown diameter (C_D), crown length (C_L) and crown projection area (C_A) as shown in Fig. 3.

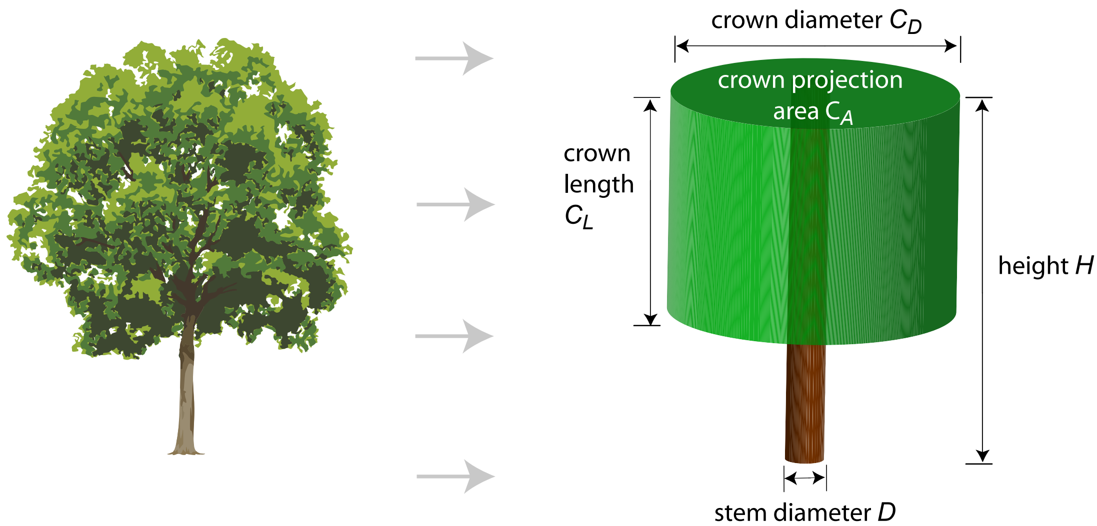

Figure 3: *Geometrical representation of a single tree . The following abbreviations describe size characteristics of the modelled tree geometry: D - stem diameter, H - height, C_D - crown diameter, C_L - crown length, C_A crown projection area.*

These size characteristics are functionally related to each other. In the following, we describe the functional relationships that can be used. Parameters of the described relationships can vary between different tree types. Some graphical examples are given in Fig. 4.

B.1 Height - Stem Diameter - Relationship

The height H [m] of a tree relates to its stem diameter D [cm] by:

Polynomial approach

$$H = h_0 + h_1 \cdot D + h_2 \cdot D^2, \tag{1}$$

where h_0, h_1 and h_2 are type-specific parameters.

Saturation approach

$$H = \frac{D}{\frac{1}{h_0} + \frac{D}{h_1}}, \tag{2}$$

where h_0 and h_1 are type-specific parameters.

Power-law approach (most frequently used)

$$H = h_0 \cdot D^{h_1}, \tag{3}$$

where h_0 and h_1 are type-specific parameters.

B.2 Crown length - Height - Relationship

The crown length C_L [m] of a tree is modelled as a fraction of its height H [m]:

Linear approach (most frequently used)

$$C_L = c_{l0} \cdot H, \tag{4}$$

where c_{l0} is a type-specific parameter.

Saturation approach

$$C_L = (-\frac{c_{l0} \cdot H \cdot c_{l1}}{c_{l0} \cdot H + c_{l1}} + c_{l2}) \cdot H, \tag{5}$$

where c_{l0}, c_{l1} and c_{l2} are type-specific parameters.

Polynomial approach

$$C_L = (c_{l0} + c_{l1} \cdot H + c_{l2} \cdot H^2) \cdot H, \tag{6}$$

where c_{l0}, c_{l1} and c_{l2} are type-specific parameters.

B.3 Crown diameter - Stem diameter - Relationship

The second dimension of the cylindrical crown, i.e. the crown diameter C_D [m] of a tree relates to its stem diameter D [cm] by:

Exponential approach I

$$C_D = D \cdot (c_{d0} + c_{d1} \cdot exp\left(-c_{d2} \cdot D\right)), \tag{7}$$

where c_{d0}, c_{d1} and c_{d2} are type-specific parameters.

Exponential approach II

$$C_D = c_{d0} \cdot D + c_{d1} \cdot exp\left(-c_{d2} \cdot D\right), \tag{8}$$

where c_{d0}, c_{d1} and c_{d2} are type-specific parameters.

Polynomial approach

$$C_D = c_{d0} + c_{d1} \cdot D + c_{d2} \cdot D^2 + c_{d3} \cdot D^3, \tag{9}$$

where c_{d0}, c_{d1}, c_{d2} and c_{d3} are type-specific parameters.

Linear approach

$$C_D = c_{d0} \cdot D, \tag{10}$$

where c_{d0} is a type-specific parameter.

Saturation approach

$$C_D = \frac{D}{\frac{1}{c_{d0}} + \frac{D}{c_{d1}}}, \tag{11}$$

where c_{d0} and c_{d1} are type-specific parameters.

Power-law approach (most frequently used)

$$C_D = c_{d0} \cdot D^{c_{d1}} - c_{d2}, \tag{12}$$

where c_{d0}, c_{d1} and c_{d2} are type-specific parameters.

B.4 Crown area - Crown diameter - Relationship

The crown projection area C_A [m^2] of a tree is simply the ground area of the modelled cylindrical crown:

$$C_A = \frac{\pi}{4} \cdot C_D^2. \tag{13}$$

B.5 Aboveground biomass - Stem diameter - Relationship

The aboveground volume of a tree captures biomass (i.e. organic dry matter). The following different ways of modelling the aboveground biomass are included in FORMIND 3.0 :

Geometrical approach (most frequently used)

Aboveground biomass B [t_{ODM}] of a tree is calculated in relation to its stem diameter D [m] and height H [m] by:

$$B = \frac{\pi}{4} \cdot D^2 \cdot H \cdot f \cdot \frac{\rho}{\sigma}, \tag{14}$$

whereby the calculation simply represents the volume of the tree stem (according to its geometry) multiplied by three factors, which describe the biomass content more concisely.

Firstly, f [-] denotes a type-specific form factor, which accounts for deviations of the stem from a cylindrical shape. Secondly, the parameter ρ [t_{ODM}/m^3] represents the wood density, which describes how much organic dry matter per unit of volume the stem contains. Thirdly, the division by the parameter σ [t_{ODM}/t_{ODM}], which represents the fraction of total aboveground biomass attributed to the stem, results then in the total aboveground biomass B.

In contrast to the constant parameters ρ and σ, the form factor f can change during the growth of an individual with respect to its stem diameter D [cm] by using either:

- $$f = f_0 \cdot exp\left(f_1 \cdot D^{f_2}\right), \tag{15}$$

  whereby f_0, f_1 and f_2 are type-specific parameters or

- $$f = f_0 \cdot D^{f_1}, \tag{16}$$

  whereby f_0 and f_1 are type-specific parameters.

Power-law approach

Aboveground biomass B [t_{ODM}] of a tree can also be modelled in relation to its stem diameter D [m] by:

$$B = b_0 \cdot D^{b_1}, \tag{17}$$

whereby b_0 and b_1 are type-specific parameters.

Logarithmic approach

Aboveground biomass B [t_{ODM}] of a tree can also be modelled in relation to its stem diameter D [cm] by:

$$B = exp\left(b_0 \cdot (log(D) - b_2) \cdot \frac{2 \cdot b_1 + (log(D) - b_2)}{b_1 + (log(D) - b_2)}\right), \tag{18}$$

whereby b_0, b_1 and b_2 are type-specific parameters.

B.6 Leaf area index - Stem diameter - Relationship

In general, aboveground biomass is divided between woody biomass captured in the stem and green biomass captured in the crown leaves. Important for the photosynthetic production of a tree is the green biomass captured in crown leaves. As leaves absorb radiation for photosynthesis, the total amount of one-sided leaf area per unit of crown projection area (i.e. the individual's leaf area index) is of main interest. The leaf area index LAI [m^2/m^2] of a tree relates functionally to its stem diameter D [cm] by:

Power-law approach (most frequently used)

$$LAI = l_0 \cdot D^{l_1}, \tag{19}$$

whereby l_0 and l_1 are type-specific parameters.

Linear approach

$$LAI = l_0 + l_1 \cdot \frac{D}{100}, \tag{20}$$

whereby l_0 and l_1 are type-specific parameters.

Fig. 4 shows all modeled functional relationships with exemplary parameters.

B.7 Maximum Values

The trees cannot grow indefinitely in FORMIND 3.0 . We introduce the following maximum values for a plausible geometry of a mature individual:

- maximum stem diameter D_{max} [m]
- maximum height H_{max} [m]

Either the maximum stem diameter or the maximum height is given as a type-specific input parameter. The missing maximum value and the corresponding maximum biomass B_{max} [t_{ODM}] are then derived using the functional relationships mentioned in section B.1 and section B.5. The maximum values are used in section F.

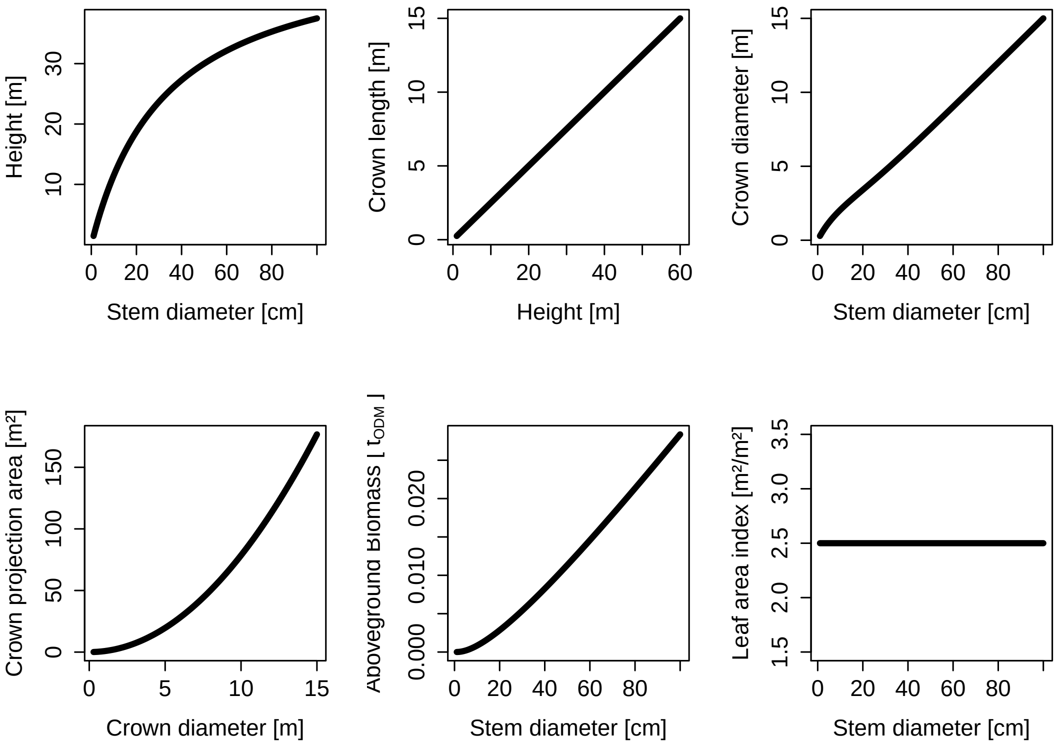

Figure 4: *Illustration of the modelled functional relationships, which are used to describe the geometry of a single tree . The approaches are in all cases the most frequently used ones. As parameters here we use the mean values of the parameter range, documented in table 2*

Table 2: *Summary of the morphological parameter range based on tropical parameterizations.*

parameter	values range	unit
$H_{\max}$	15 - 55	m
h_0	2 - 7	-
h_1	0.2 - 0.7	-
c_{l0}	0.3 - 0.4	-
c_{d0}	0.5 - 0.6	-
c_{d1}	0.65 - 0.75	-
c_{d2}	0.0 - 0.3	-
ρ	0.4 - 0.8	$\frac{todm}{m^3}$
σ	0.7	$\frac{todm}{todm}$
f_0	0.75 - 0.80	-
f_1	-0.15 - -0.20	-
l_0	1 - 3	-
l_1	0.1 - 0.3	-

C Recruitment and Establishment

FORMIND 3.0 includes two different possibilities to model recruitment:

- by using global constant in-growth rates or
- by seed production and dispersal of mother trees.

C.1 Global in-growth rates

The number of recruited seeds is assumed to be brought into the local community from an intact forest community surrounding the simulated area. This number N_{seed} [$^1/_{\text{yr ha}}$] is thereby a constant type-specific parameter independent of the density of individuals already existing on the simulated area.

The recruited seeds directly enter the seed pool, but they may only germinate and establish in the next time step. Each patch is assigned an own seed pool. The recruited seeds are distributed uniformly across the patches and added to the corresponding seed pool in an amount of:

$$N_{pool} = \left\lfloor \frac{N_{seed}}{\#patches} \right\rfloor . \tag{21}$$

If the number of ingrowing seeds N_{seed} is not a multiple of the number of patches $\#patches$, a certain number of seeds will remain which are distributed randomly to the patches. For this, the patches are considered one by one incrementally starting with the first. Within each considered patch and for each remaining seed, which has not been distributed yet, its probability of assignment to the currently considered patch is compared with a random number (uniformly distributed in [0;1]). In the case of successful assignment (i.e. random number $\leq 1/\#patches$), the seed number per patch N_{pool} is incremented and the number of remaining seeds decremented. At the end, the last patch receives all remaining seeds.

Before the start of the simulation, N_{init} seeds already existing in the seed pool per patch (i.e. $N_{pool} = N_{init}$) can be defined for each type, which may germinate and establish as seedlings already in the first time step.

C.2 Seed production and dispersal of mother trees

Before the start of the simulation, it is obligatory to assign to the seed pool of each patch a type-specific number of seeds N_{init}.

During the simulation, each individual of a cohort per patch is able to produce a predefined type-specific number of seeds N_{seed} on its own as a mother plant if it reaches a predefined stem diameter D_{rep}. These produced seeds are dispersed among the neighboring patches surrounding that patch the mother plant is located in. The dispersal is dependent on a defined dispersal kernel, the crown diameter C_D of the mother plant and a predefined type-specific average dispersal distance $dist$.

There is no distinction between different dispersal agents (e.g. wind, birds, mammals). The dispersal kernel is assumed to be Weibull distributed with a shape parameter of 2 and a scale parameter of $(dist + C_D/2)^2$. Presuming rotation symmetry, the probability density f_{disp} that seeds are dispersed at a distance r from the mother plant is defined as:

$$f_{disp}(r) = \frac{2 \cdot r}{\left(dist + \frac{C_D}{2}\right)^2} \cdot e^{-\frac{r^2}{\left(dist+\frac{C_D}{2}\right)^2}}. \tag{22}$$

For each seed per mother plant per patch, a distance r is stochastically drawn from the dispersal kernel $f_{disp}(r)$. Using the calculated distance r and a random direction DIR (drawn from a uniform distribution in the range of [0°;360°]), the target coordinates of the dispersed seed are determined in the following way:

$$x_{seed} = x_{ind} + r\ sin\left(2\ \pi\ \frac{DIR}{360}\right) \tag{23}$$

$$y_{seed} = y_{ind} + r\ cos\left(2\ \pi\ \frac{DIR}{360}\right) \tag{24}$$

whereby (x_{ind}, y_{ind}) is a randomly generated position of the mother plant within its corresponding patch and (x_{seed}, y_{seed}) is the calculated virtual position of the dispersed seed on the simulation area. As in FORMIND 3.0 individuals do not have spatially explicit positions within the patches, the corresponding patch number of the dispersed seed is calculated from the coordinates (x_{seed}, y_{seed}).

The sum of those produced seeds, which are dispersed to a certain patch are added first to its corresponding seed pool N_{pool} before they are able to germinate and establish in the next time step.

C.3 Germination of seeds

Before seeds can germinate from the seed pool and establish successfully, light and space conditions are checked. Per type a minimum number of seeds can be withheld in the seed pool, which is by default set to 0.

For determining the light conditions, the incoming irradiance on the floor is divided by the incoming irradiance above canopy (see section E for their calculation). This results in the percentage of incoming irradiance on the floor I_{floor}, which is possibly reduced due to shading of already existing individuals. Dependent on a minimum percentage of light I_{seed} required for seed germination and seedling establishment for each type, it is checked whether I_{floor} is sufficient:

$$N_{germ} = \begin{cases} N_{pool} & ,I_{floor} \geq I_{seed} \\ 0 & ,I_{floor} < I_{seed} \end{cases}, \tag{25}$$

whereby N_{germ} is the number of germinated seedlings.

If light requirements are not sufficient for seeds of a specific type, they remain in the seed pool and may germinate in future time step as far as conditions become favorable. By this, seeds may accumulate in the seed pool if light conditions remain unfavorable over a period of time.

Seeds waiting in the seed pool for favorable germination conditions may be affected by seed pool mortality. For each type a mortality rate M_{pool} [$^1/_{\mathrm{yr}}$] is defined prior to the start of the simulation. A rate of $M_{pool} = 0$ represents, for example, an unlimited accumulation of seeds in times of unfavorable conditions. In contrast, a rate of $M_{pool} = 1$ would not allow any accumulation of seeds in the seed pool.

The density of germinated seedlings can be additionally regulated. Thereby, for each type and patch the number N_{germ} is truncated at a predefined value max_{dens}.

C.4 Establishment of seedlings

If light requirements are fulfilled for successful seedling germination, it is secondly checked whether enough space is available for their establishment. Germinated seedlings start with a predetermined stem diameter D_{min}, irrespective of type or species. Using the chosen functional relationships describing the geometry of an individual (see section B), their corresponding height H_{min} can be calculated. If space at the respective height is already filled by more than 100% with existing individuals, none of the germinated seedlings would be able to establish:

$$N_{est} = \begin{cases} N_{germ} & ,CCA_l < 1 \\ 0 & ,CCA_l \geq 1 \end{cases}, \tag{26}$$

whereby N_{est} is the number of successfully established seedlings and CCA_l denotes the cumulative crown area at the height layer l (of width Δh [m]) which correspond to H_{min}:

$$l = \left\lfloor \frac{H_{min}}{\Delta h} \right\rfloor . \tag{27}$$

See section D for the calculation of the cumulative crown area CCA of all height layer of the aboveground discretized space.

D Mortality

In FORMIND 3.0 trees can die due to various reasons. The following different types of mortality occur in a serial way:

- background mortality M_B
- mortality dependent on an individual's stem diameter M_D
- mortality dependent on an individual's diameter increment M_I
- crowding mortality due to limited space
- mortality due to damage by a falling tree
- mortality due to fragmentation

Individual trees of the same type and size, which are located in the same patch, are summarized in this section by a so-called **cohort**. Each cohort is uniquely described by its type, the number of identical trees (N), their age and the size of one single tree (i.e. aboveground biomass). In this section, the number of identical trees in a cohort change due to mortality processes. In the following, we describe the different types of mortality in more detail.

D.1 General mortality

In contrast to the later described event-driven forms of mortality, there is a general mortality rate per tree which is active in each time step t_y. This mortality rate M is calculated as the sum of the background mortality rate M_B and two further mortality rates dependent on the stem diameter M_D as well as its increment M_I:

$$M = M_B + M_D + M_I. \tag{28}$$

The background mortality M_B [$^1/_{\mathrm{yr}}$] is a type-specific constant input parameter.

The mortality rate M_D depends on the stem diameter D [m] and provides the possibility to give older trees (with a bigger stem diameter) a higher mortality rate than younger trees or vice versa. The rate is calculated by:

$$M_D(D) = m_{d0} \cdot D^{m_{d1}}, \tag{29}$$

whereby m_{d0} and m_{d1} are type-specific parameters.

The mortality rate M_I depends on the increment of the stem diameter D [mm] per time step t_y and provides the possibility to include a higher mortality for older trees or those under stress. It is modelled by the functional relationship:

$$M_I(\Delta D) = m_{i0} + m_{i1}\ \Delta D + m_{i2} \Delta D^2, \tag{30}$$

where m_{i0}, m_{i1} and m_{i2} are type-specific parameters. The increment of the stem diameter from time t to time $t + t_y$ is denoted as ΔD.

The trees per patch die according to their mortality rate M - either stochastically or deterministically.

Deterministic dying is active if the number of individuals per cohort is greater than a predefined number N_M **<u>and</u>** if the stem diameter of each individual is smaller than a predefined threshold D_M. In this case, the number of dying trees per cohort is determined by:

$$N_Y = N \cdot M, \tag{31}$$

where N is the number of trees per cohort, N_Y is the number of dying trees per cohort and M is the calculated mortality rate per time step t_y. The number of dying trees N_Y is rounded by $\lfloor N_Y + 0.5 \rfloor$.

In the contrary case (i.e. $N < N_M$ **or** $D > D_M$), deaths occur stochastically. That means, for each tree the mortality rate M represents its probability of dying (i.e. by comparing a random number from a uniform distribution in the range of [0;1] with the mortality rate M):

$$N_Y = \sum_{j=1}^{N} \delta_{rM}, \tag{32}$$

where N is the number of trees per cohort, N_Y is the number of dying trees per cohort, M is the calculated mortality rate per time step t_y and r is a random number from a uniform distribution in the range of [0;1]. The symbol δ_{rM} is defined as:

$$\delta_{rM} = \begin{cases} 1 & , r \leq M \\ 0 & , r > M \end{cases} \tag{33}$$

D.2 Crowding mortality

Crowding occurs, if at any height layer the cumulative crown area of all trees on a patch exceeds A_{patch}. At first, the cumulative crown area CCA [m^2/m^2] of all trees on a patch is calculated for each height layer i relative to the patch area A_{patch}:

$$CCA_i = \frac{1}{A_{patch}} \cdot \sum_{\substack{all\ individuals \\ with\ l_{min} \leq i \leq l_{max}}} C_A, \tag{34}$$

where C_A is the crown projection area of a tree (see section B). Thereby, each tree occupies only a limited amount of height layers (i.e. between layer l_{min} and l_{max}) defined by the individual's crown length C_L [m] and its height H [m]:

$$l_{max} = \left\lfloor \frac{H}{\Delta h} \right\rfloor \tag{35}$$

$$l_{min} = \left\lfloor \frac{H - C_L}{\Delta h} \right\rfloor \tag{36}$$

Mortality due to crowding is calculated per tree represented by a reduction factor R_c [-]. This individual reduction factor is calculated based on those height layers, which the individual's crown is occupying (Fig. 5).

The reduction factor R_c is determined by the reciprocal of the maximum cumulative crown area according to those height layers between the individual limits l_{min} and l_{max}:

$$R_c = \frac{1}{\max\limits_{i \in [l_{min};l_{max}]} (CCA_i)}. \tag{37}$$

If the maximum cumulative crown area of any height layer, which the individual's crown is occupying, exceeds A_{patch} (i.e. $CCA_i > 1$), the individual reduction factor R_c falls below the threshold of 0.99. In this case, the number of dying identical trees per cohort N_C is calculated by:

$$N_C = N\ (1 - R_c). \tag{38}$$

Mortality due to crowding (or self-thinning) can be interpreted as competition for space. Besides crowding, the vertical discretization of the aboveground space is also important for the light climate calculations. To save computation time, the calculation of R_c is coupled to that of the light climate which is explained in chapter E.

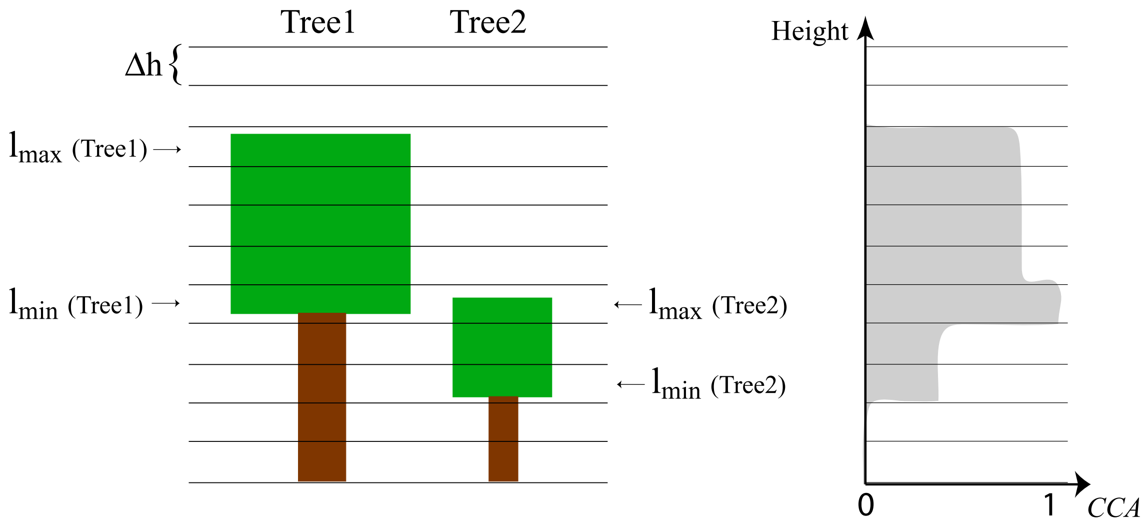

Figure 5: *Illustration of crowding on the example of two single trees . The limits of each crown are shown by l_{min}(Tree1), l_{max}(Tree1), l_{min}(Tree2) and l_{max}(Tree2). The vertically discretized aboveground space into height layers of width Δh [m] is coloured differently according to the sum of the crown projection areas of both individuals occupying the layers. The darker the colour is, the more crowns occupy the respective height layer. This is calculated by the cumulative crown area CCA [-] relative to the patch area, which is illustrated on the right side. The maximum of CCA is used to calculate the reduction factor R_c for each individual. In this example, the reduction factor for each of both trees is calculated based on the 5. height layer from the bottom (equal to layer l_{min}(Tree1) and l_{max}(Tree2)).*

D.3 Tree fall mortality

If a tree falls, neighboring trees can be destroyed. A dying tree falls down with probability f_{fall}. The falling target patch depends on falling direction and on tree height H. Falling direction DIR (drawn from a uniform distribution in the range of [0°, 360°]) is chosen randomly. The target coordinates of the falling tree (x_{fall}, y_{fall}) are determined in the following way:

$$x_{fall} = x_{tree} + H\ sin\left(2\ \pi\ \frac{DIR}{360}\right) \tag{39}$$

$$y_{fall} = y_{tree} + H\ cos\left(2\ \pi\ \frac{DIR}{360}\right) \tag{40}$$

whereby (x_{tree}, y_{tree}) is the standing position of the falling tree . With this target coordinates the affected patch is determined. All smaller trees (tree height $< H$) in this target patch are dying with a damage rate M_{dam}:

$$M_{dam} = C_A / A_{patch}, \tag{41}$$

whereby C_A is the crown area of the falling tree and A_{patch} the area of the target patch.

The trees in the target patch die according to the damage rate M_{dam} - either stochastically or deterministically. Deterministic dying is active if the number of trees per cohort is greater than 100. In this case, the number of dying trees per cohort N_F is determined by multiplying number of trees N per cohort with damage rate M_{dam}.

$$N_F = N \cdot M_{dam}, \tag{42}$$

The number of dying trees N_F is rounded by $\lfloor N_F + 0.5 \rfloor$.

In the contrary case (less than 100 trees per cohort), stochastic dying is performed. That means, for each tree the damage rate M_{dam} represents its probability of dying (i.e. by comparing a random number from a uniform distribution in the range of $[0; 1]$ with the damage rate).

$$N_F = \sum_{j=1}^{N} \delta_{rM_{dam}}, \tag{43}$$

where N is the number of trees per cohort, N_F is the number of dying trees per cohort, M_{dam} is the damage rate per time step t_y and r is a random number from a uniform distribution in the range of $[0; 1]$. The symbol $\delta_{rM_{dam}}$ is defined as:

$$\delta_{rM_{dam}} = \begin{cases} 1 & , r \leq M_{dam} \\ 0 & , r > M_{dam} \end{cases} \tag{44}$$

D.4 Change of mortality due to fragmentation

It has been observed that mortality is increased and tree species richness is reduced at forest edges, and that large trees are often missing in small fragments (Ferreira and Laurance, 1997; Laurance et al., 1998b, Arroyo-Rodriguez and Mandujano, 2006; Laurance et al., 2000, Pimentel Lopes de Melo et al. 2006). The extent of forest edges varies between forest regions. For example, increased edge mortality could be measured up to 100 m into the forest interior in the Amazon (Ferreira and Laurance, 1997).

In FORMIND 3.0 we model increased mortality at the edge of forest fragments by multiplying the general mortality M with a fragmentation variable m_{frag}. Thus, the additional mortality due to fragmentation can be calculated as:

$$M_{frag} = M \cdot (m_{frag} - 1). \tag{45}$$

We assume that the fragmentation induced mortality M_{frag} is higher at forest edges (< 100 m) than in the interior. Thus, the value of m_{frag} is modelled dependent on the distance to the fragment edges (Tab. 3). In addition, large trees ($D > 60$ cm) can suffer an increased mortality.

Table 3: *Mortality increase due to fragmentation, dependent on the distance to a fragment edge and on the stem diameter D [cm] of a tree .*

Distance to edge	Value of m_{frag} ($D \leq 60$)	Value of m_{frag} ($D > 60$)
0 - 20 m	2.5	4
20 - 40 m	1.75	2.5
40 - 60 m	1.375	1.75
60 - 80 m	1.1875	1.375
80 - 100 m	1.09375	1.1875

If this type of mortality is activated, we recommend to choose a patch size of 20 m x 20 m (i.e. $A_{patch} = 400\ \ \mathrm{m}^2$) according to the distance classes in Table 3.

The number of additional trees that die due to fragmentation effects can be calculated as:

$$N_{frag} = N \cdot M_{frag}. \tag{46}$$

D.5 Overall change in number of trees per cohort

Overall, per time step Δt and for each cohort the change in the number of trees per cohort N is determined by:

$$dN/dt = -(N_Y + N_C + N_F + N_{frag}), \tag{47}$$

where N_Y is the number of trees dying due to regular mortality, N_C is the number of trees dying due to crowding, N_F is the number of trees dying due to damages caused by a falling tree and N_{frag} is the number of trees dying due to increased mortality near fragment edges.

The amount of above ground carbon S_{mort} [$^{tC}/_{ha}$], which results from the death of trees within the current time step is calculated by:

$$S_{mort} = 0.44 \cdot \sum_{all\ cohorts} (N_Y + N_C + N_F + N_{frag}) \cdot B, \tag{48}$$

where B is the above ground biomass of the tree (see section B). We assume that 1 g organic dry matter contains 44 % carbon [Larcher, 2001].

E Competition and environmental limitations

E.1 Light climate

A single tree on a patch receives full incoming radiation. An increasing number of individual trees of differing heights on a patch results in shading within the canopy. Higher trees intercept radiation, which is not available for smaller individuals. Thus, with decreasing height from the canopy down to the ground, radiation is decreasing. We call this vertical distribution of light availability within a patch 'light climate'.

To calculate the light availability in different heights within the canopy, the vertical discretization of the above-ground space is used (i.e. height layers of constant width Δh). For each patch and height layer, the leaf area accumulated by all trees on the patch is calculated. Each tree contributes parts of its crown leaf area to those height layers, which are occupied by its crown (i.e. height layers from l_{min} to l_{max}). These limits are determined by the individual's crown length C_L and its height H:

$$l_{max} = \left\lfloor \frac{H}{\Delta h} \right\rfloor \tag{49}$$

$$l_{min} = \left\lfloor \frac{H - C_L}{\Delta h} \right\rfloor . \tag{50}$$

The number of height layers a tree is occupying by its crown (n_{layer}) can then be calculated by:

$$n_{layer} = l_{max} - l_{min}. \tag{51}$$

For those height layers between l_{min} and l_{max}, an individual's leaf area contributes equally to each layer i:

$$\bar{L}_i = \frac{LAI \cdot C_A}{n_{layer}}, \tag{52}$$

whereby $\bar{L}_i$ [m^2] represents the contribution of an tree 's leaf area to the layer i, LAI [-] is the leaf area index of the tree (see section B.6) and C_A [m^2] is crown projection area of the tree 's crown. The multiplication of LAI by C_A results in the leaf area in [m^2] of an single tree .
Summing up all contributions of the trees ' leaf area per patch to their respective occupied height layers and relative to the patch area, results in the patch-based leaf area index $\hat{L}_i$ [-] per layer i:

$$\hat{L}_i = \frac{1}{A_{patch}} \sum_{\substack{all\ individuals \\ with\ l_{min} \le i \le l_{max}}} \bar{L}_i, \tag{53}$$

where $\bar{L}_i$ [m^2] represents the leaf area contribution of an tree to the height layer i and A_{patch} [m^2] denotes the area of a patch.

Using this information, the radiation each tree is able to intercept can be determined. Light attenuation through the canopy is calculated using the approach of [Monsi and Saeki, 1953]. The incoming radiation I_{ind} on top of a tree (i.e. on top of the height layer l_{max} the tree is reaching) is calculated by:

$$I_{ind} = I_0 \cdot exp\left(-k \cdot \sum_{i>l_{max}} \hat{L}_i\right), \tag{54}$$

where the sum in the exponent accumulates the patch-based leaf area indices of all height layers above the individual's height. The parameter k denotes the light extinction coefficient [-] of a tree , I_0 [μmol (photons)/m^2 s] is the daily radiation above canopy averaged from sunrise to sunset during the vegetation period and $\hat{L}_i$ [-] represents the patch-based leaf area index of height layer i.

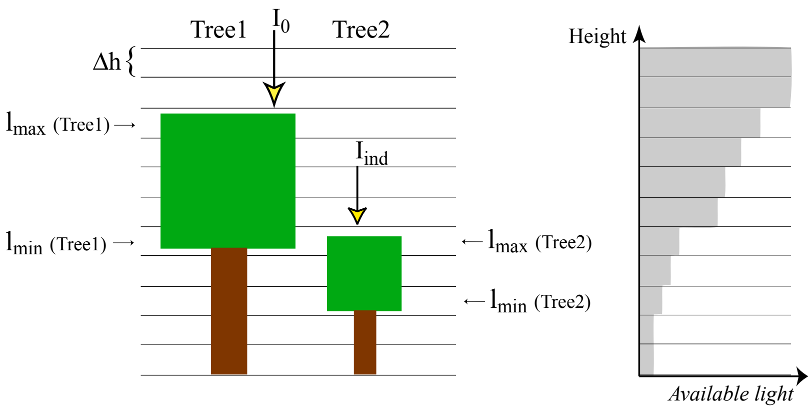

Figure 6: *Illustration of the light climate on the example of two single trees . The limits of each crown are shown by l_{min} (Tree1), l_{max}(Tree1), l_{min}(Tree2) and l_{max}(Tree2). The vertically discretized aboveground space into height layers of width Δh [m] is coloured differently according to the available radiation. The lighter the colour is, the more attenuated the radiation is, which results from the absorption by higher individuals' leaves. On the right hand side the decrease of available light from the canopy to the floor is illustrated by the grey polygon. Thereby, attenuation is greatest in the height layer both trees occupy by their crowns (i.e. layer l_{min}(Tree1) and l_{max}(Tree2)).*

By determining the available radiation for each single tree (at the top of the crown), competition for light between trees is considered.

E.2 Water cycle and soil water limitation

Individual trees take up soil water resources to fulfill the requirements for their gross productivity. We determine an individual's uptake of soil water based on its demand and on the total available soil water.

Firstly, the soil water content Θ_{soil} is computed preliminary on an hourly basis using a differential equation, which quantifies preliminary hourly changes in the soil water content per patch depending on precipitation PR, interception IN and run-off RO (Fig. 7, cf. [Kumagai et al., 2004]):

$$\frac{d\Theta_{soil}}{dt} = PR(t) - IN(t) - RO(t). \tag{55}$$

The resulting soil water content represents the total available soil water before soil water uptake by individuals. Uptake of soil water resources by trees is modelled equal to their transpiration and subtracted from Θ_{soil} later within the timestep (see eqn. 66).

The **interception** IN [mm/h] is calculated dependent on the total leaf area index per patch (i.e. $\sum_i \hat{L}_i$ in [-], cf. [Liang et al., 1994]):

$$IN(t) = min(K_L \cdot \left(\sum_i \hat{L}_i\right), PR(t)), \tag{56}$$

where K_L [mm/h] is the interception constant and PR [mm/h] denotes the precipitation.

On the ground surface of a patch, we consider two different run-offs: surface run-off and subsurface run-off:

$$RO(t) = RO_{\rightarrow}(t) + RO_{\downarrow}(t), \tag{57}$$

where **surface run-off** $RO_{\rightarrow}$ [mm/h] is defined in the following way:

$$RO_{\rightarrow} = max(0, \Theta_{soil}(t) + PR(t) - IN(t) - POR) \tag{58}$$

with POR [mm/h] denoting the soil porosity (i.e. defined as the maximum water intake of the soil per patch).All additional incoming water is assumed to be surface run-off.

For the calculation of the **subsurface run-off** $RO_{\downarrow}$ due to gravitation, we use the Brooks-Corey relation (cf. [Liang et al., 1994]):

$$RO_{\downarrow} = K_s \cdot \left(\frac{\Theta_{soil}(t) - \Theta_{res}}{POR - \Theta_{res}}\right)^{\frac{2}{\lambda}+3}, \tag{59}$$

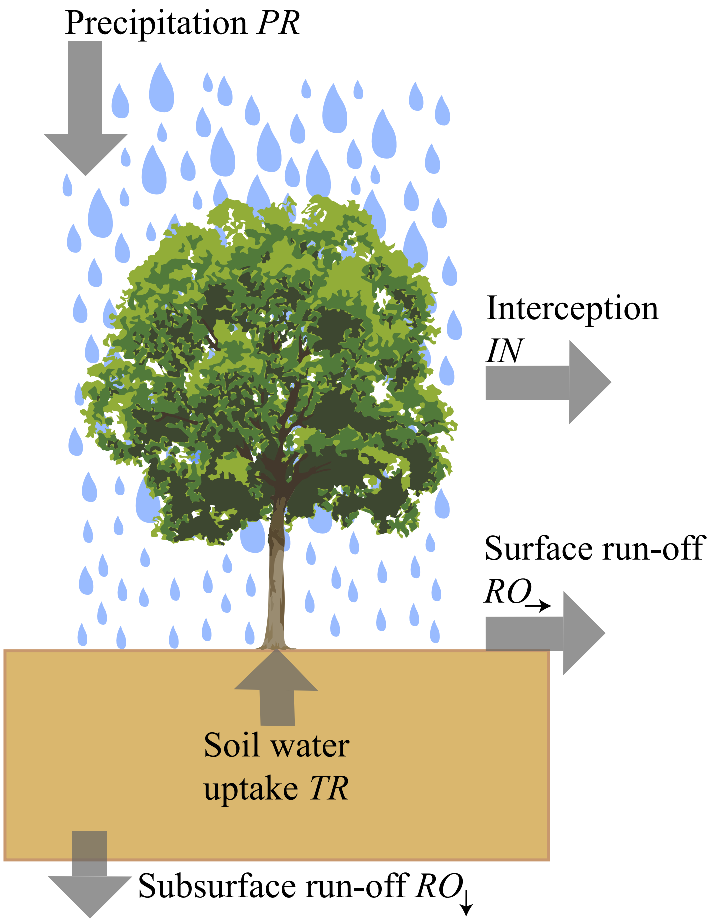

Figure 7: *Illustration of the water cycle on the example of a single tree .*

where K_s [mm/h] is the fully saturated conductivity, Θ_{res} [mm/h] the residual water content, and λ [-] the pore size distribution index.

The preliminary soil water content Θ_{soil} represents the soil water content, which is available for the individuals' uptake or transpiration. To calculate the **transpiration** TR [mm/h] of all trees per patch, we use the water-use-efficiency concept (cf. [Lambers et al., 2008]):

$$TR = \frac{1}{A_{patch}} \sum_{all\ trees} \frac{GPP}{WUE}, \tag{60}$$

whereby GPP in $[g_{ODM}/\mathrm{h}]$ denotes the hourly gross primary production of an individual on the patch (see section F). Please note, that we simulate GPP per time step t_y. To calculate GPP on an hourly basis, we divide GPP $[g_{ODM}/\Delta t]$ by the number of hours within the time step Δt. The constant type-specific value WUE in $[g_{ODM}/kg_{H_2O}]$ represents the water-use-efficiency parameter and A_{patch} [m^2] the area of a patch.

The resulting transpiration TR may be limited in three ways calculated in a serial way:

PET limitation Transpiration can be limited by the potential evapotranspiration PET [mm/h] and the interception IN [mm/h] (calculated by eqn. 56):

$$TR_{new} = \begin{cases} TR(t) & , TR(t) \leq PET(t) - IN(t) \\ PET(t) - IN(t) & , TR(t) > PET(t) - IN(t) \end{cases}. \tag{61}$$

Soil water limitation Transpiration can be limited by the preliminary soil water content Θ_{soil} [mm/h] (calculated by eqn. 55) and the permanent wilting point Θ_{pwp} [mm/h]:

$$TR_{new}(\Theta_{soil}) = \begin{cases} TR(t) & ,\Theta_{soil}(t) - TR(t) \geq \Theta_{pwp} \\ \Theta_{soil}(t) - \Theta_{pwp} & ,\Theta_{soil}(t) - TR(t) < \Theta_{pwp} \\ 0 & ,\Theta_{soil}(t) \leq \Theta_{pwp} \end{cases}. \tag{62}$$

Competition for water Competition between trees can limit the transpiration in the following way:

$$TR = \varphi_W(\Theta_{soil}) \cdot TR(t), \tag{63}$$

where φ_W [-] represents a reduction factor ranging between 0 and 1, depending on the actual soil water content.

The reduction factor φ_W is calculated using the approach of [Granier et al., 1999], which is based on the preliminary soil water content (calculated by eqn. 55):

$$\varphi_W(\Theta_{soil}) = \begin{cases} 0 & ,\Theta_{soil}(t) \leq \Theta_{pwp} \\ \frac{\Theta_{soil}(t)-\Theta_{pwp}}{\Theta_{msw}-\Theta_{pwp}} & ,\Theta_{pwp} < \Theta_{soil}(t) < \Theta_{msw} \ , \\ 1 & ,\Theta_{soil}(t) \leq \Theta_{msw} \end{cases} \tag{64}$$

where Θ_{pwp} is the permanent wilting point in $[V\%]$ and Θ_{msw} is the minimum soil water content in $[V\%]$. For the purpose of the calculation of eqn. 64 only, Θ_{soil} needs to be converted from [mm/h] to [V%]. Thereby, the soil is modelled down to a constant depth [m] defined prior to the start of the simulation.

The minimum soil water content (Θ_{msw}) is determined according to [Granier et al., 1999] by:

$$\Theta_{msw} = \Theta_{pwp} + 0.4(\Theta_{fc} - \Theta_{pwp}) \tag{65}$$

whereby Θ_{fc} denotes the field capacity in $[V\%]$.

The soil water content in the next day step is then calculated by the difference between the preliminary soil water content (calculated by eqn. 55) and the (eventually limited) transpiration TR:

$$\frac{d\Theta_{soil}}{dt} = \Theta_{soil}(t)–TR(t). \tag{66}$$

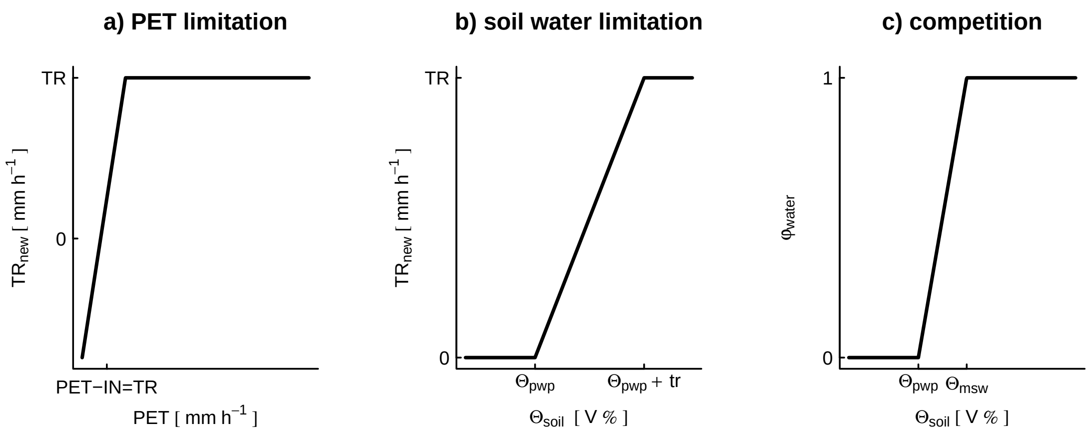

Figure 8: *Water limitation function. a) limitation of TR due to PET. b) limitation of TR due to Soil water. c) φ_{water} as function of Soil water.*

E.3 Temperature

The gross primary production GPP $[t_{ODM}/t_y]$ of a tree (see section F) may be influenced by phenology (esp. in the temperate zone) and air temperature. Respiration for maintenance purposes of an individual (see section F) may also be affected by air temperature. The influence on both - gross productivity and respiration, is modelled using limitation factor, by which they are simply multiplied (see section F). In the following, we describe the calculations of these limitation factors:

Phenology

Individual trees make photosynthesis only during their photosynthetic active period. In the **temperate zone**, we distinguish between broad-leaf and needle-leaf trees . Only deciduous broad-leaf trees have two phenology phases: (i) a dormant phase during winter and (ii) a photosynthetic active period of φ_{act} [days] after bud-burst until fall (i.e. the vegetation period).

The date of bud-burst is reached, if the temperature sum (daily mean air temperatures $> 5°$) since 1 January is higher than a critical temperature T_{crit} [Sato et al., 2007]:

$$T_{crit} = -68 + 638\ e^{-0.01 \cdot n}, \tag{67}$$

where n is the number of days per time step Δt with an air temperature below 5° since 1 November of the previous year. This algorithm is based on the global distribution of leaf onset dates estimated from remote sensing data [Botta et al., 2000]. The photosynthetic active period stops if the 10-day moving average of daily mean air temperatures falls below $9°C$ [Sato et al., 2007].

In contrast to the broad-leaf trees, the photosynthetic active period φ_{act} of needle-leaf trees amounts a complete year of 365 days (without any dormant phase).

In the **tropical zone**, we assume for all individuals irrespective of their type a complete photosynthetic active period with $\varphi_{act} = 365$ days.

Temperature limitation of gross productivity

The gross primary production of a tree can be reduced due to air temperatures. A corresponding limitation factor φ_T is calculated by averaging the reduction factors over the whole time step Δt:

$$\varphi_T = \frac{1}{n} \sum_{1}^{n} \varphi_{T,l} \cdot \varphi_{T,h}, \tag{68}$$

where n is the number of days per time step Δt and the values $\varphi_{T,l}$ and $\varphi_{T,h}$ are the daily inhibition factors for low and high air temperatures [Gutiérrez and Huth, 2012; Haxeltine and Prentice, 1996].

The **reduction factor for low air temperatures** $\varphi_{T,l}$ $[°C]$ is calculated by:

$$\varphi_{T,l} = \left(1 + e^{k_0 \cdot k_1 - T}\right)^{-1}, \tag{69}$$

where T $[°C]$ is the daily mean air temperature and k_0 and k_1 are type-specific parameters.

These parameters k_0 and k_1 are calculated by:

$$k_0 = \frac{2\ ln(0.01/0.99)}{T_{CO_2,l} - T_{cold}} \tag{70}$$

$$k_1 = 0.5\ (T_{CO_2,l} + T_{cold}) \tag{71}$$

where $T_{CO_2,l}$ $[°C]$ and T_{cold} $[°C]$ are type-specific parameters representing the lowest temperature limit for CO_2 assimilation and the monthly mean air temperature of the coldest month an individual can cope with, respectively.

Similarly, the **inhibition factor for high air temperatures** $\varphi_{T,h}$ in $°C$ is calculated by:

$$\varphi_{T,h} = 1 - 0.01 \cdot e^{k_2\ (T - T_{hot})} \tag{72}$$

where k_2 is a type-specific parameter, T $[°C]$ is the daily mean temperature and T_{hot} $[°C]$ is the type-specific mean temperature of the hottest month an individual can occur.

The parameter k_2 is calculated as:

$$k_2 = \frac{ln(0.99/0.01)}{T_{CO_2,h} - T_{hot}}, \tag{73}$$

whereby $T_{CO_2,h}$ $[°C]$ and T_{hot} $[°C]$ are type-specific parameters representing the higher temperature limit for CO_2 assimilation and the monthly mean air temperature of the warmest month an individual can cope with, respectively.

Temperature limitation of maintenance respiration

Maintenance respiration is assumed to change exponentially with air temperature represented by the limitation factor κ_T [Prentice et al., 1993]:

$$\kappa_T = \frac{1}{n} \sum_{1}^{n} Q_{10}^{\left(\frac{T - T_{ref}}{10}\right)}, \tag{74}$$

where n is the number of days per time step t_y, T [$°C$] is the daily mean air temperature, Q_{10} [-] and T_{ref} [$°C$] are constant parameters, irrespective of type. T_{ref} represents the reference temperature, at which maintenance respiration is not influenced. Air temperatures below T_{ref} result in a decrease of maintenance respiration ($\kappa_T < 1$) and those above T_{ref} in an increase of maintenance respiration ($\kappa_T > 1$).

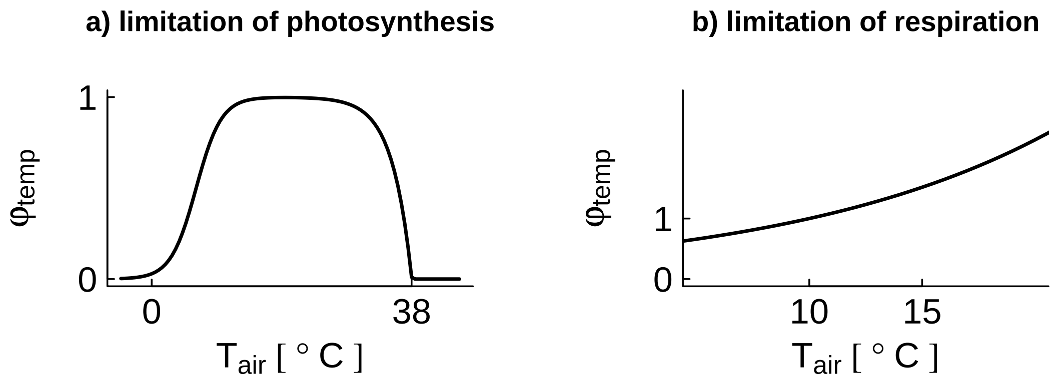

Figure 9: *Temperature limitation function. a) limitation factor of Photosynthesis. b) limitation factor of maintenance respiration.*

F Growth of a tree

F.1 Interim photosynthesis

Based on the incoming irradiance on top of a tree I_{ind} (see section E), organic dry matter is produced via gross photosynthesis. In this section the interim photosynthesis is calculated without reduction due to limited soil water availability nor temperature effects.

The interim gross photosynthesis P_{ind} of an individual is modelled using the approach of [Thornley and Johnson, 1990]. It is based on the single-leaf photosynthesis modelled by a Michaelis-Menten function – a typical saturation function describing the relation between the radiation I_{leaf} available on top of a leaf and its gross photosynthetic rate P_{leaf}:

$$P_{leaf}(I_{leaf}) = \frac{\alpha \cdot I_{leaf} \cdot p_{max}}{\alpha \cdot I_{leaf} + p_{max}}, \tag{75}$$

where α is the quantum efficiency, also known as the initial slope of the type-specific light response curve, I_{leaf} is the incoming irradiance on top of the surface of a single leaf within the individual's crown and p_{max} is the maximum leaf gross photosynthetic rate.

To obtain the incoming irradiance on top of the surface of a single leaf I_{leaf}, the available irradiance I_{ind} on top of the entire individual has to be modified:

$$I_{leaf}(L) = \frac{k}{1-m}\, I_{ind} \cdot e^{-k \cdot L}, \tag{76}$$

where k [-] is the type-specific light extinction coefficient, m [-] represents the transmission coefficient and I_{ind} denotes the available incoming irradiance on top of a tree .

The first part $\frac{k}{1-m}\, I_{ind}$ in eqn. (76) is correcting the incoming irradiance in order to obtain those parts, which can be absorbed by a leaf. The second part $e^{-k \cdot L}$ in eqn. (76) accounts for self-shading within the individual's crown. As the leaves of an individual are assumed to be homogeneously distributed within its crown, some leaves will be shaded by higher ones within the crown. Thereby, $L = 0$ represents the top of the individual and $L = LAI$ represents the bottom of the individual's crown with LAI being its leaf area index (see section B).

To obtain the interim gross photosynthetic rate of a tree per year P_{ind}, the single-leaf photosynthesis of eqn. (75) is integrated over the individual's leaf area index LAI (see section B):

$$P_{ind} = \int_0^{LAI} P_{leaf}(I_{leaf}(L))dL. \tag{77}$$

The integration results in the interim photosynthesis of an tree per year [Thornley and Johnson, 1990]:

$$P_{ind} = \frac{p_{max}}{k} \cdot ln \frac{\alpha\ k\ I_{ind} + p_{max}(1-m)}{\alpha\ k\ I_{ind}\ e^{-k \cdot LAI} + p_{max}(1-m)}. \tag{78}$$

To convert the interim photosynthesis P_{ind} from $[\mu mol_{CO_2}/m^2 s]$ to $[t_{ODM}/y]$, P_{ind} has to be multiplied by the individual's crown area C_A (see section B), the type-specific photosynthetic active period φ_{act} and finally a conversion factor c_{odm}:

$$P_{ind} \cdot C_A \cdot 60 \cdot 60 \cdot l_{day} \cdot \varphi_{act} \cdot \varphi_{odm}, \tag{79}$$

where the multiplication by $60 \cdot 60$ accounts for the conversion from seconds to hours. The factor l_{day} [h] represents the mean day length during the vegetation period φ_{act} [d] (see section E). The conversion factor $\varphi_{odm} = 0.63 \cdot 44 \cdot 10^{-12}$ includes the molar mass of CO_2, the conversion from g to t and the conversion from CO_2 to organic dry mass ODM [Larcher, 2001].

F.2 Gross primary production

The gross primary production GPP of a tree is calculated from the interim photosynthesis P_{ind} $[t_{ODM}/y]$ (see section F.1):

$$GPP = P_{ind}\ \varphi_T\ \varphi_W, \tag{80}$$

where φ_W denotes the reduction factor accounting for limited soil water and φ_T represents the limitation factor of air temperature effect. Both factors range between 0 and 1 and thus, only reducing GPP in times of unfavorable conditions (see section E).

F.3 Biomass increment of a tree

Gross primary production GPP of eqn. (80) is first used for the maintenance of the already existing aboveground biomass of an tree . Costs for maintenance are modelled as biomass losses in terms of maintenance respiration R_m $[t_{ODM}/y]$. The remaining productivity $(GPP - R_m)$ is then available for growth of new aboveground biomass. Costs for the production of new structural tissue are modelled also as biomass losses in terms of growth respiration. This results in the net productivity ΔB [Dislich et al., 2009]:

$$\Delta B = (1 - r_g)\ (GPP - R_m), \tag{81}$$

where r_g [-] represents a constant parameter describing the fraction of $(GPP - R_m)$ attributed to growth respiration. In contrast, maintenance respiration R_m is modelled proportionally to the already existing aboveground biomass of a tree (see section F.4).

F.4 Maintenance respiration

The maintenance respiration R_m of a tree is calculated inversely by rearranging eqn. (81):

$$R_m = GPP - \frac{\Delta B}{1 - r_g}. \tag{82}$$

Maintenance respiration R_m is further modelled proportional to the already existing aboveground biomass B [t_{ODM}] of an individual:

$$R_m = \kappa_T \cdot r_m \cdot B, \tag{83}$$

where r_m denotes the maintenance respiration rate [$^1/_y$] and κ_T represents a limitation factor dependent on air temperature (see section E).

Combining equation (82) with equation (83) and arranging in terms of the respiration rate r_m results in:

$$r_m = \frac{1}{B \cdot \kappa_T} \cdot \left(GPP - \frac{\Delta B}{1 - R_g} \right). \tag{84}$$

In FORMIND 3.0 we have two different approaches of calculating the maintenance respiration rate based on eqn. (84):

- Optimal approach (no limitation)
- Observation-based approach

In the following, we describe both approaches in more detail.

Optimal approach (most frequently used)

The maintenance respiration rate r_m of eqn. (84) is calculated using the assumption of full resource availability. Thereby, it is assumed that full resource availability (i.e. no limitation by shading, soil water or air temperature) results in the observed maxima of field measurements of stem diameter increments:

$$r_m = \frac{1}{B} \cdot \left(P_{ind}(I_0) - \frac{B(D + g(D)) - B}{(1 - R_g)} \right), \tag{85}$$

where this equation can be obtained by substituting in eqn. (84) (i) κ_T by 1, (ii) GPP by the gross productivity under full resource availability $P_{ind}(I_0)$ (see eqn. 79) with I_0 as the full available incoming irradiance and (iii) ΔB by the biomass increment derived from the maximum stem diameter increment under full resource availability $D + g(D)$ using the individual's geometry (see section B). See section F.5 for different modelling approaches of the *maximum diameter growth curve* $g(D)$.

This approach is proposed when climate data at the time of field measurements are not available.

Observation-based approach

In this approach, the maintenance respiration rate r_m is calculated including those climatic conditions, which were observed during the field measurements of stem diameter increments. The correspondence of environmental factors (see section E) to these climatic conditions during the observations is indicated by $\check{()}$.

$$r_m = \frac{1}{B} \cdot \left(GPP(\check{I_{ind}}, \check{\varphi_{act}}, \check{\varphi_T}, \check{\varphi_W}) - \frac{B(D + g(D)) - B}{(1 - R_g)} \right), \tag{86}$$

where this equation can be obtained by substituting in eqn. (84) (i) κ_T by 1, (ii) GPP by the gross productivity under the climate during observations $GPP(\check{I_{ind}}, \check{\varphi_{act}}, \check{\varphi_T}, \check{\varphi_W})$ and (iii) ΔB by the biomass increment derived from the maximum stem diameter increment using the individual's geometry $D + g(D)$ (see section B). See section F.5 for different modelling approaches of the *maximum diameter growth curve* $g(D)$.

This approach is proposed when climate data are available at the time field data on stem diameter increments were measured. In general, diameter increments are determined based on the difference of stem diameter measurements between two dates. For this time period climate data would be needed on which the limitation factors $\check{I_{ind}}$, $\check{\varphi_{act}}$, $\check{\varphi_T}$ and $\check{\varphi_W}$ of eqn. (86) can be calculated as described in section E.

F.5 Maximum diameter growth curve

In the field, diameter increments can be determined by calculating the differences between two measurements of the stem diameter per tree (at two distinct observation dates). The increments are then usually plotted with the measured stem diameter of the first observation date to get an impression of how much a tree of stem diameter D is able to increase (see Fig. 10 for an example).

Such point clouds as illustrated in Fig. 10 can be described by functional relationships. Please note, that you have to adjust the increments according to a time step of 1 year. That means, if there is a period of e.g. 5 years between both observation dates of stem diameter measurements, you would have to correct the increments with respect to the smaller time scale.

In FORMIND 3.0 we have two different approaches of determining the diameter growth function $g(D)$:

- Calculation of coefficients from curve characteristics

- Coefficients as input parameter

In the following we describe both approaches in more detail.

Calculation of coefficients from curve characteristics

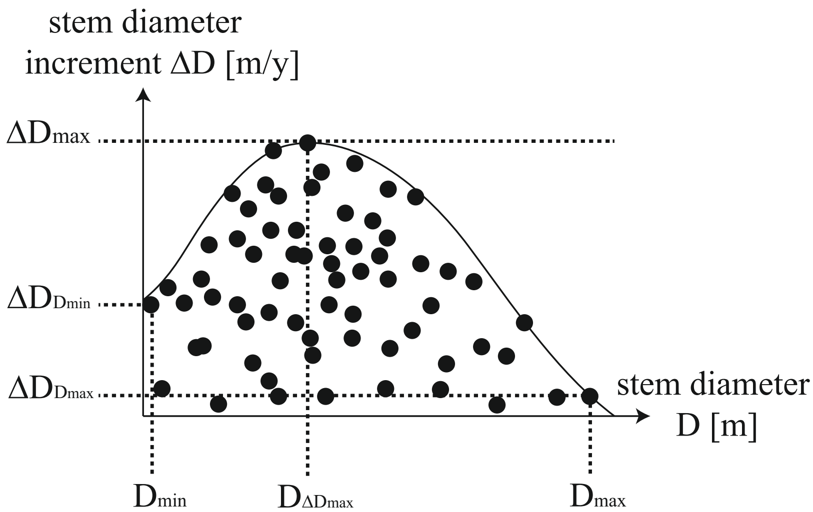

Figure 10: *Illustration of a measured diameter growth curve. Points represent illustrative measurements. The solid line represents a fitted growth function to the maximum values of the measurements. Dotted lines show important characteristics which would be needed for the first approach.*

Only a few information of the measured diameter increment curve are needed to derive:

- maximum diameter increment ΔD_{max} [m/y]
- stem diameter $D_{\Delta D_{max}}$ [% of D_{max}], which reaches ΔD_{max}
- maximum diameter increment $\Delta D_{D_{min}}$ [% of ΔD_{max}] of the smallest possible tree (with $D = D_{min}$)
- maximum diameter increment $\Delta D_{D_{max}}$ [% of ΔD_{max}] of the biggest possible tree (with $D = D_{max}$)

Based on these characteristics, the coefficients of the growth function $g(D)$ can be calculated explicitly. Two different growth function are available:

- Polynomial approach
- Chanter approach

In the following, we show for both functional approaches of $g(D)$ the calculation of their coefficients.

Polynomial approach

The polynomial approach describes the growth function $g(D)$ as a polynom of third degree:

$$g(D) = a_0 + a_1 \cdot D + a_2 \cdot D^2 + a_3 \cdot D^3, \tag{87}$$

where a_0,a_1,a_2 and a_3 are the type-specific coefficients, which are calculated as follows:

$$\begin{aligned}
a_3 &= \frac{(x_0 \cdot x_1 + (\Delta D_{D_{min}} - \Delta D_{D_{max}}) \cdot \Delta D_{max} \cdot x_2)}{x_3 + x_4 + x_5 + x_6 + x_7} \\
a_2 &= \frac{(x_0 - a_3 \cdot x_8)}{(2 \cdot D_{min} \cdot (D_{\Delta D_{max}} \cdot D_{max}) - (D_{\Delta D_{max}} \cdot D_{max})^2 - D_{min}^2)} \\
a_1 &= -3 \cdot a_3 \cdot (D_{\Delta D_{max}} \cdot D_{max})^2 - 2 \cdot a_2 \cdot (D_{\Delta D_{max}} \cdot D_{max}) \\
a_0 &= \Delta D_{D_{min}} \cdot \Delta D_{max} - a_3 \cdot D_{min}^3 - a_2 \cdot D_{min}^2 - a_1 \cdot D_{min}
\end{aligned}$$

with

$$\begin{aligned}
x_0 &= \Delta D_{max} - \Delta D_{D_{min}} \cdot \Delta D_{max} \\
x_1 &= 2 \cdot (D_{\Delta D_{max}} \cdot D_{max}) \cdot (D_{min} - D_{max}) - D_{min}^2 + D_{max}^2 \\
x_2 &= 2 \cdot (D_{\Delta D_{max}} \cdot D_{max}) \cdot (D_{min} - (D_{\Delta D_{max}} \cdot D_{max})) - D_{min}^2 + (D_{\Delta D_{max}} \cdot D_{max})^2 \\
x_3 &= (D_{\Delta D_{max}} \cdot D_{max})^4 \cdot (D_{max} - D_{min}) \\
x_4 &= 2 \cdot (D_{\Delta D_{max}} \cdot D_{max})^3 \cdot (D_{min}^2 - D_{max}^2) \\
x_5 &= (D_{\Delta D_{max}} \cdot D_{max})^2 \cdot (5 \cdot D_{min}^3 + 3 \cdot D_{min} \cdot D_{max}^2 - 3 \cdot D_{max} \cdot D_{min}^2 + D_{max}^3) \\
x_6 &= 2 \cdot (D_{\Delta D_{max}} \cdot D_{max}) \cdot (D_{max} \cdot D_{min}^3 - D_{min} \cdot D_{max}^3) \\
x_7 &= D_{max}^3 \cdot D_{min}^2 - D_{max}^2 \cdot D_{min}^3 + D_{min}^4 - D_{min}^5 \\
x_8 &= 3 \cdot D_{min} \cdot (D_{\Delta D_{max}} \cdot D_{max})^2 - 2 \cdot (D_{\Delta D_{max}} \cdot D_{max})^3 - D_{min}^3
\end{aligned}$$

Chanter approach

This approach describes the growth function $g(D)$ as follows:

$$g(D) = a_0 \cdot D \cdot \left(1 - \frac{D}{D_{max}}\right) \cdot e^{-a_1 \cdot D}, \tag{88}$$

where a_0 and a_1 are the type-specific coefficients, which are calculated by:

$$\begin{aligned} a_0 &= \frac{e^{\frac{D_{max} - 2 \cdot (D_{\Delta D_{max}} \cdot D_{max})}{D_{max} - (D_{\Delta D_{max}} \cdot D_{max})}} \cdot D_{max} \cdot \Delta D_{max}}{(D_{max} - (D_{\Delta D_{max}} \cdot D_{max})) \cdot (D_{\Delta D_{max}} \cdot D_{max})} \\ a_1 &= \frac{D_{max} - 2 \cdot (D_{\Delta D_{max}} \cdot D_{max})}{D_{max} \cdot (D_{\Delta D_{max}} \cdot D_{max}) - (D_{\Delta D_{max}} \cdot D_{max})^2}, \end{aligned}$$

whereby D_{max} is calculated out of maximum height (see section B.7).

Coefficients as input parameter

For this approach, the coefficients of the corresponding growth function $g(D)$ are input parameter already known prior to the start of the simulation. The following three different functional approaches of $g(D)$ are implemented:

Weibull approach

The growth function $g(D)$ is described by a Weibull function of:

$$g(D) = a_0 \cdot a_1 \cdot a_2 \cdot (a_1 \cdot D)^{a_2 - 1} \cdot e^{-(a_1 \cdot D)^{a_2}}, \tag{89}$$

where a_0, a_1 and a_2 are the type-specific coefficients.

Richards approach

The growth function $g(D)$ is described by:

$$g(D) = a_0 \cdot a_1 \cdot a_2 \cdot e^{-a_1 \cdot D} \cdot \left(1 - e^{-a_1 \cdot D}\right)^{a_2 - 1}, \tag{90}$$

where a_0, a_1 and a_2 are the type-specific coefficients.

Chanter approach (most freqeuntly used)

The growth function $g(D)$ is described by:

$$g(D) = a_0 \cdot D \cdot \left(1 - \frac{D}{D_{max}}\right) \cdot e^{-a_1 \cdot D}, \tag{91}$$

where a_0 and a_1 are the type-specific coefficients.

Please note, when determining the type-specific coefficients prior to the start of the simulation, that the curve represents growth under full resource availability. That means, not all measurements should be fitted, but only the maximum diameter increments (see Fischer, 2010 p. 55 for an example).

G Disturbance

Disturbances comprise the following scenarios:

- fire events, which affect trees depending on their fire resistance
- landslide events, which create bare soil

In total, N_D individuals of a cohort are dying due to disturbance induced mortality events.

G.1 Fire

Fire is the primary disturbance process affecting the terrestrial biosphere [Pfeiffer et al., 2013]. Especially wildfires affect species composition and vegetation structure in forests. They lead to a decrease of carbon storage and result in the emission of greenhouse gases. There is a long tradition in fire ecology to understand these processes and their interactions. Numerous methods were developed to estimate the disturbances due to fire events. Fire events are a complex distubances, which can be described by fire frequency, fire area and severity.

To understand the effect of fire on vegetation dynamics and vegetation structure, we developed the forest fire module ForFire, which is a combination of the ideas of well-established fire models [Gardner et al., 1999; Keane et al., 2004; Thonicke et al., 2001]. External inputs to the ForFire module are the mean fire frequency per hectare and year (λ in [years]), the mean fire size related to the investigated forest area (β in [%]) and the mean fire severity (s_{fire} [0-1]). Fire events are implemented on the patch level, i.e. the smallest possible fire size has the size of one patch (A_{patch}), the biggest fire considered are all patches of the simulation area.

- **fire events:** We implemented fire events in the following way: in every year a random number determines the number of fire events within this year. This fire frequency is poisson distributed [Green, 1989] with λ as mean time between fire events. If a fire event occurs, the fire centre is chosen randomly within the simulated forest area. The fire size (equal to the number of burned patches) is described by an exponential distribution β as mean size of the fire area related to the whole simulated forest area [Green, 1989]. The fire spread is modelled randomly: (i.) going from the fire centre every neighboring patch is burned, (ii.) a randomly burned patch is chosen and (iii.) again every neighboring patch is burned. This procedure is repeated until the number of the burned patches is equal to the specified fire size.

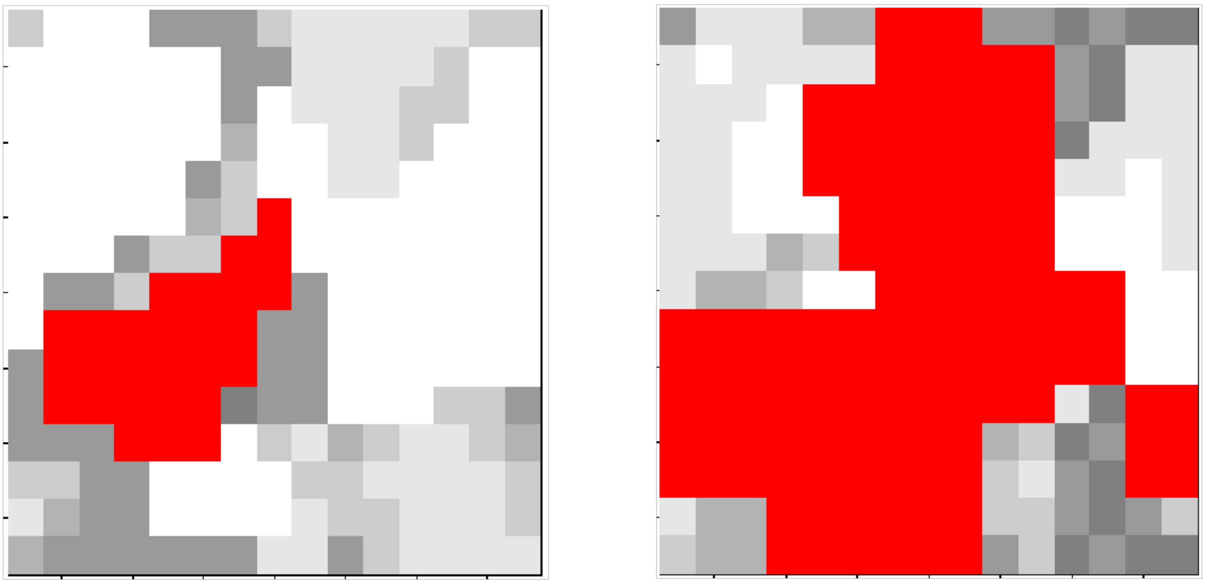

Figure 11: *Visualization of two randomly chosen fire events. The simulated area is nine hectare. The grey level indicates the amount of standing biomass. The red colour shows the fire spread.*

- **fire tolerance of trees:** According to the fire tolerance of a tree species, not every tree is burning and dying in the fire area. The probability for tree burning depends on fire tolerance of the species, on the stem diameter (D [cm]) as a proxy of tree age and on the fire severity [Busing and Solomon, 2006]. We distinguish between four fire tolerance levels for tree species. Tree species of level 1 are dying in a fire, independent of stem diameter or fire severity. Tree species with a fire tolerance up to level 4 have an increasing fire-resistance. The burning probability for every tree is calculated as follows depending on the fire tolerance of the tree species [Busing and Solomon, 2006]:

$$
\begin{aligned}
P_{F1} &= 1 \\
P_{F2} &= e^{((-(1-s_{fire})\cdot 0.00202)-0.00053)\cdot D} \\
P_{F3} &= e^{((-(1-s_{fire})\cdot 0.02745)-0.00255)\cdot D} \\
P_{F4} &= e^{-0.00053\cdot D} - 0.5 - (1-s_{fire})\cdot 0.5
\end{aligned}
$$

where s_{fire} (value between 0-1) is an indicator for the severity and the type of the fire (Fig. 12) and D is the stem diameter.

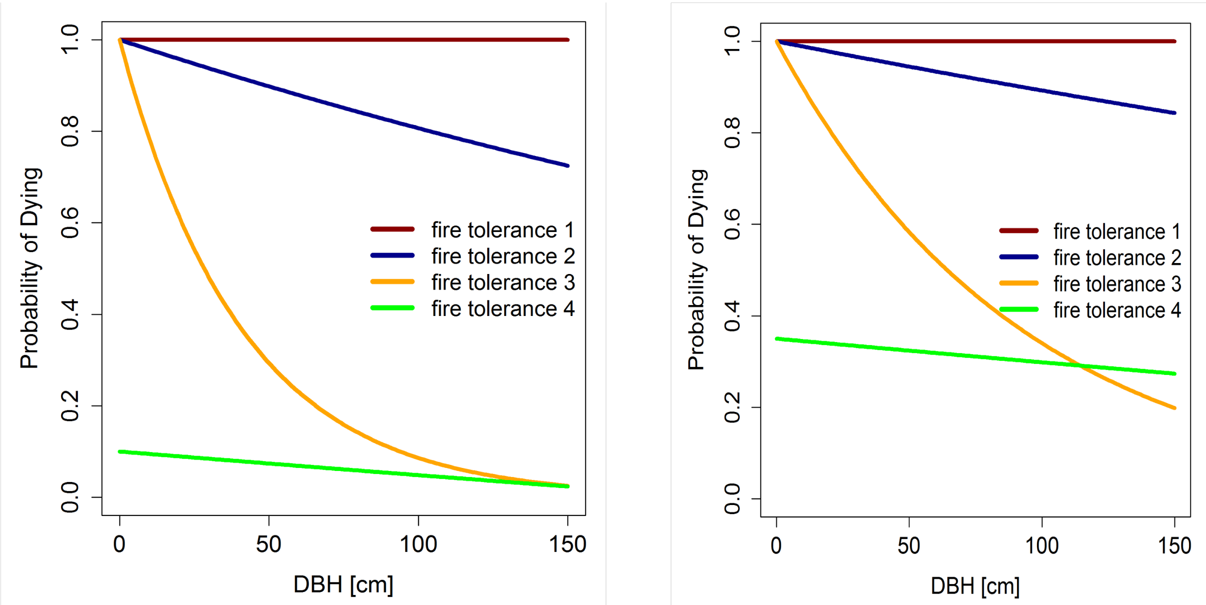

Figure 12: *Probability for tree dying after a fire event depending on stem diameter (D) and fire tolerance group. Left: probability of dying after a weak fire event (s_{fire}=0.2). Right: probability of dying after a strong fire event (s_{fire}=0.7).*

G.2 Landslides

In montane forests shallow landslides can constitute a recurring natural disturbance. Disturbance by landslides differs from disturbances by falling trees or logging in the sense that all vegetation, as well as upper soil layers and seed bank are removed from the disturbed patch. Forest regeneration on landslide surfaces therefore underlies particular environmental conditions. For instance, solar radiation on recent landslide sites is high and nutrient levels of landslide soils are low [Wilcke et al., 2003]. Due to this changed environmental conditions, establishment rates of trees as well as tree mortality and tree growth rates might deviate from the basic type-specific rates.

To study potential effects of landslide disturbances on the forest carbon cycle and species composition, we implemented landslides as a particular type of disturbance into the FORMIND 3.0 model. External inputs to the landslide module are the landslide frequency per hectare and year (*slidefreq*) and the distribution of landslide sizes. Landslide disturbance is implemented on the patch level, i.e. the smallest possible landslide has the size of one patch A_{patch} (i.e. 20 m x 20 m) and the biggest landslides considered are for example 25 patches (1 hectare).

We implemented landslides in the following way: for each hectare and in every year a randomly drawn number determines whether a landslide occurs (probability f_{land}). Since the annual frequency on a per hectare basis will usually be small, we do not account for multiple landslides on one hectare in the same year. The size of the landslide is drawn from a size distribution (s) of landslides, rounded for the patch size A_{patch}. The starting location of the landslide is a random patch and the directionality of landslides is always the same. Neighbouring patches of the starting location are affected until the slide reaches the predetermined size.

All trees in landslide affected patches die and are removed from the patch. Since recruiting trees in FORMIND 3.0 have a stem diameter of D_{min} [cm] at breast height, there is a time lag (t_{lag}) between the landslide event and the occurrence of the first trees on the slide surface. Based on the potential growth of trees this time lag can be estimated for the different tree types. Forest recovery then proceeds according to one of the following scenarios: undisturbed regrowth, reduced growth, reduced recruitment, increased mortality. For the justification of these scenarios, see [Dislich and Huth, 2012]

- **Undisturbed regrowth:** All type-specific parameters stay unchanged. This situation considers increased light levels after the landslide disturbance but neglects additional environmental changes.

All other scenarios describe a temporal change in type-specific traits. The underlying assumption is that the strongest change in traits occurs immediately after the landslide and traits come back to their normal level, as forest recovery proceeds after the disturbance. The parameter r_{land} represents the assumed change in tree species attributes after landslide occurrence.

- **Reduced growth:** FORMIND 3.0 calculates tree growth as biomass increment per year (ΔB, cf. section F.3). Assuming a simple linear relation between growth reduction and 'recovery status' of the disturbed site, which is expressed by the ratio of accumulated dead biomass (B_{dead}) to the minimum biomass in a mature patch (B_{mat}), the reduced biomass increment (ΔB_{red}) is calculated via:

$$\Delta B_{red}(B_{dead}) = \left(r_{land} \cdot \frac{B_{dead}}{B_{mat}} + (1 - r_{land}) \right) \cdot \Delta B. \tag{92}$$

- **Reduced recruitment:** The type-specific recruitment rate per hectare and year (N_{seed}, cf. section C) might be changed due to landslide disturbances. Like in the reduced growth scenario, we assume a linear relationship between the amount of recruitment reduction and recovery status of the patch, now expressed by the ratio of established biomass in the recovering patch (B_{pat}) to the minimum biomass of a mature patch (B_{mat}). Therefore the reduced recruitment rate (N_{red}) is calculated via:

$$N_{red}(B_{pat}) = \left(r_{land} \cdot \frac{B_{pat}}{B_{mat}} + (1 - r_{land}) \right) \cdot N_{seed} \tag{93}$$

- **Increased mortality:** The type-specific mortality rate (M) might change due to landslide disturbance (cf. section D). Again, we assume a linear relationship between the increment in mortality rate and the recovery status of the patch, represented by the ratio of established biomass in the recovering patch (B_{pat}) to the minimum biomass of a mature patch (B_{mat}). Therefore the increased mortality rate (M_{inc}) is calculated as:

$$M_{inc}(B_{pat}) = \left(1 + \left(r_{land} - r_{land} \cdot \frac{B_{pat}}{B_{mat}} \right) \right) \cdot M. \tag{94}$$

The choice of the parameter r_{land} as well as the chosen functional relationship between changed attributes and recovery state of the successional forest is adapted according to site specific knowledge. Exemplary values for the parameters t_{lag}, r_{land} and f_{land} are shown in table 4 and 5. The slide side distribution is given in 6

Table 4: *Exemplary values for the time lag parameter t_{lag} [Dislich and Huth, 2012].*

Type	t_{lag}
pioneer species	3
mid-successional species	5
climax species	12

Table 5: *Exemplary values for the parameters r_{land} and f_{land} [Dislich and Huth, 2012].*

Parameter	Value
r_{land}	0.9, 0.5
f_{land}	0.02

Table 6: *Exemplary slide size distribution s [Dislich and Huth, 2012].*

Landslide size [m^2]	Frequency
400	0.30
800	0.26
1200	0.16
1600	0.09
2000	0.08
2400	0.03
2800	0.03
3200	0.01
3600	0.03
4000	0.005
4400	0.005
$\geq$ 4800	0

H Carbon cycle

The calculation of the carbon cycle in FORMIND 3.0 uses a simple compartment approach consisting of the following explicit carbon stocks:

- living forest stock, which equals the amount of carbon of alive trees
- deadwood stock S_{dead}, which equals the amount of carbon of dead trees
- slow decomposing soil stock S_{slow}, which accounts for the slow decomposing share of carbon in the deadwood stock
- fast decomposing soil stock S_{fast}, which accounts for the fast decomposing share of carbon in the deadwood stock

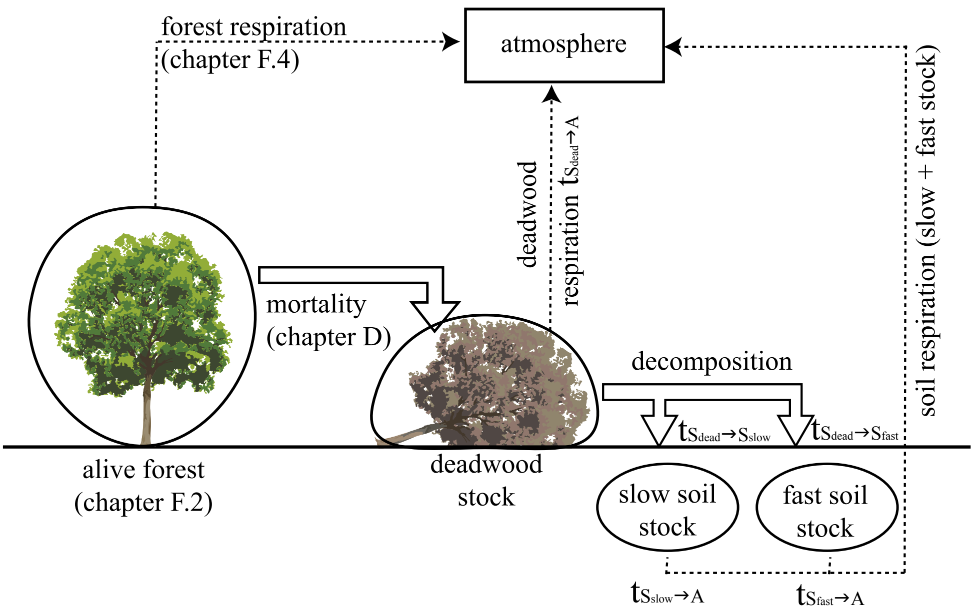

Figure 13: *Schematic visualization of the carbon cycle in FORMIND 3.0 . Circles represent explicit carbon stocks and the rectangle indicates the atmosphere. Dotted arrows show carbon released to the atmosphere from the respective stock and block arrows show carbon transitions between the respective explicit carbon stocks.*

The dynamics of the living forest stock (i.e. carbon storage in form of growth and carbon releases as respiration) are described earlier in section F. The dynamics of the remaining stocks is described by a set of differential equations:

$$\begin{aligned}
\frac{\mathsf{d}S_{dead}}{\mathsf{d}t} &= S_{mort} - (t_{S_{dead}\to A} + t_{S_{dead}\to S_{slow}} + t_{S_{dead}\to S_{fast}}) \cdot S_{dead} \\
\frac{\mathsf{d}S_{slow}}{\mathsf{d}t} &= t_{S_{dead}\to S_{slow}} \cdot S_{dead} - t_{S_{slow}\to A} \cdot S_{slow} \\
\frac{\mathsf{d}S_{fast}}{\mathsf{d}t} &= t_{S_{dead}\to S_{fast}} \cdot S_{dead} - t_{S_{fast}\to A} \cdot S_{fast}
\end{aligned}$$

where the parameters $t_{S_{dead}\to A}$, $t_{S_{slow}\to A}$ and $t_{S_{fast}\to A}$ denote transition rates in [$^1/\mathrm{yr}$] of released carbon from the respective soil stocks to the atmosphere. The parameter $t_{S_{dead}\to S_{slow}}$ and $t_{S_{dead}\to S_{fast}}$ represent in turn decomposition rates of deadwood material in [$^1/\mathrm{yr}$]. The variable S_{mort} [$^{tC}/\mathrm{ha}$] represents the carbon of all trees dying within the current time step (see section D).

H.1 Determining the transition rates

The transition rates depend on how fast microorganisms can decompose the fallen litter or dead trees. For describing the decomposition rates, we use an approach presented earlier by Sato et al. [2007]. The annual decomposition rate $t_{S_{dead}\to}$ for the deadwood stock is calculated as follows:

$$t_{S_{dead}\to} = \min\left(1.0, \frac{10^{-1.4553+0.0014175\cdot AET}}{12}\right), \tag{95}$$

where AET is considered as the actual evapotranspiration in the previous year in mm. The variable AET is calculated by the sum of interception IN and transpiration TR (cf. section E.2).

The annual decomposition rate $t_{S_{dead}\to}$ is modelled as the sum of all transitions rates of the deadwood pool S_{dead}:

$$t_{S_{dead}\to} = t_{S_{dead}\to A} + t_{S_{dead}\to S_{slow}} + t_{S_{dead}\to S_{fast}} \tag{96}$$

According to [Sato et al., 2007] 70 % of the carbon of decomposing deadwood biomass (i.e. litter) is directly released to the atmosphere, while the remaining 30 % are transferred to the slow and fast decomposing soil stocks. In detail, 98.5 % of the remaining carbon is transferred to the fast soil stock and 1.5 % to the slow soil stock. We then calculate the specific transition rates as follows:

$$\begin{aligned} t_{S_{dead} \to A} &= 0.7 \cdot t_{S_{dead} \to} \\ t_{S_{dead} \to S_{slow}} &= 0.015 \cdot 0.3 \cdot t_{S_{dead} \to} \\ t_{S_{dead} \to S_{fast}} &= 0.985 \cdot 0.3 \cdot t_{S_{dead} \to} \end{aligned}$$

H.2 The Net Ecosystem Exchange (NEE)

The NEE is the carbon net flux of the forest. We define the NEE $[{}^{tC}/_{\mathrm{ha\ yr}}]$ as follows:

$$NEE = C_{GPP} - C_R - t_{S_{dead} \to A} \cdot S_{dead} - t_{S_{slow} \to A} \cdot S_{slow} - t_{S_{fast} \to A} \cdot S_{fast}, \tag{97}$$

where S_{dead} $[{}^{tC}/_{\mathrm{ha}}]$ denotes the deadwood carbon pool, S_{slow} $[{}^{tC}/_{\mathrm{ha}}]$ and S_{fast} $[{}^{tC}/_{\mathrm{ha}}]$ the soil carbon stock (i.e. slow and fast decomposing), $t_{x \to A}$ $[{}^{1}/_{\mathrm{yr}}]$ the corresponding transition rates of released carbon from the respective stock x resulting from the microbiological respiration (cf. section H) and C_{GPP} $[{}^{tC}/_{\mathrm{ha\ yr}}]$ is the carbon captured in the gross primary productivity of the living forest (cf. section F.2), C_R $[{}^{tC}/_{\mathrm{ha\ yr}}]$ is the carbon released by the total respiration of the living forest (i.e. for maintenance and growth). We also assume here that 1 g organic dry matter contains 44 % carbon, which results in:

$$\begin{aligned} C_{GPP} &= 0.44 \cdot \sum_{all\ trees} GPP \\ C_R &= 0.44 \cdot \sum_{all\ trees} (R_m + R_g \cdot (GPP - R_m)). \end{aligned}$$

If the NEE is positive (i.e. $NEE > 0$), the forest is considered to be a carbon sink. If the NEE is negative (i.e. $NEE < 0$), the forest is considered to be a carbon source.

I Logging

Commercial trees are logged on selected areas. Trees with specific attributes are removed from the forest plot. At the same time, surrounding trees are damaged based on the chosen logging strategy, logging intensity, logging cycle, cutting limits and resulting damage [?Huth et al., 2005].

I.1 Logging strategy

The two logging strategies L_S that are provided in FORMIND, arise from different commercial and economical interests. The two strategies differ in the falling direction of a logged tree:
The reduced impact logging (RIL) takes into account a substantial planning of the logging scenario. This scenario is implemented into FORMIND by defining the falling direction of a tree towards the biggest gap. Thereby, the falling tree causes a reduced amount of damage to surrounding trees.
The conventional logging (CON) takes into account the usage of heavy machinery, unskilled workers and low to no planing strategies. This is implemented into FORMIND by a random falling direction of logged trees. The random direction causes the possibility of higher damage to surrounding trees.

I.2 Logging intensity

The logging intensity is defined by the minimum number of trees harvested within the forest plot L_{Nmin} [-] and the maximum number of trees L_{Nmax} [-].

I.3 Logging cycle

The first logging scenario is defined as L_{start} [y]. The logging cycle is the time between logging events L_C [y].

I.4 cutting limit

Commercial trees are are only logged if their dbh exceed a minimum dbh L_Dmin.

I.5 logging intensity

Logging intensity is defined as the number of remaining commercial trees in the forest after the logging event L_{remain}.

I.6 damage

The induced damage to surrounding trees depends on the dbh of the logged tree - bigger trees cause more damage to surrounding trees than smaller trees. Therefore, a percental damange L_dam is defined for four different diameter classes L_dc.

J Lidar simulation

FORMIND 3.0 allows the simulation of a Lidar scan of the forest stand at each time step. The Lidar simulator generates point clouds of discrete returns as they are usually produced by small-footprint Lidar systems.

J.1 Entities, state variables and scales

The basic entities in the model are trees, Lidar pulses and Lidar returns. Trees are characterized by their position (X- and Y-coordinate), height, crown length, crown radius and crown shape (spheroid, cone or cylinder). Modeled Lidar pulses are all perfectly vertical with regular spacing between them. Thus a Lidar pulse is only characterized by its X- and Y-coordinate. Lidar returns are points in 3 dimensional space, characterized by their X-, Y- and Z-coordinate. The model works in a 3D space represented by an array of cubic voxels of a certain side length. The resolution is determined by the voxel side length, which can be chosen according to the desired spacing of Lidar pulses, as each pulse is simply represented by one vertical column of voxels.

J.2 Process overview and scheduling

In the model at first a voxel representation of the entire forest is created. This means the value of each voxel in the 3D array that falls into a tree crown or trunk of any given tree in the input list is set to one (tree voxel). All other voxels, representing free space that is not occupied by trees get the value zero, except for the forest floor ($Z = 0$), where each voxel gets the value one. Whether a voxel becomes a tree voxel or not depends on the tree parameters position, height, crown dimensions and shape. Precise tree positions within each 20 m x 20 m patch are assigned randomly but consistent with other FORMIND 3.0 outputs, e.g. the stand visualization file. The voxel forest is hereafter scanned with a virtual Lidar. Each vertical column of voxels is considered one Lidar pulse, which can cause multiple returns. The returns are collected for each X-Y-coordinate-combination in the array.

J.3 Design concepts

The Lidar simulation follows a probabilistic approach. Instead of explicitly simulating the branches and foliage and their interaction with laser beams within the tree crowns, the model assumes that the tree crown space is a homogeneous, turbid medium. The probability to get a Lidar return from a certain point decreases with increasing distance that the laser beam has to travel through the medium before reaching that point. This is analogous to the light-extinction law after Lambert-Beer, which is also used for the light climate simulation. The only difference is that the classical Lambert-Beer equation serves to calculate remaining light intensity depending on distance, while in the discrete Lidar case the same equation is used to calculate probability P_{Lid} for a discrete return here.

$$P_{Lid}(d_{Lid}) = P_{0,Lid} \cdot e^{-k_{Lid} \cdot d_{Lid}} \tag{98}$$

Returns can only exist in tree and ground voxels. Distance d_{Lid} that the beam has to travel through crown space before reaching a focal voxel is quantified from the count of tree voxels above the focal voxel in the same array column. $P_{0,Lid}$ represents the probability to get a return from the very upper voxel, where the laser beam hits the surface (tree or ground) for the first time. The parameter k_{Lid} is the exponential extinction coefficient, which determines how fast the return probability decreases after entering the crown space. The final decision for each voxel whether it will contain a return or not is taken stochastically, based on the calculated return probability. Model outputs are tables that contain the coordinates of all tree voxels and all Lidar returns. Parameters $P_{0,Lid}$ and k_{Lid} can be set independently for vegetation ($P_{0,Lid,V}$, $k_{Lid,V}$) and ground ($P_{0,Lid,G}$, $k_{Lid,G}$) voxels to adapt to the different reflectance of the forest floor. Further parameters to run the FORMIND 3.0 Lidar simulator are the pulse spacing s_{Lid} and the time interval between successive scans t_{Lid}. The Lidar simulation works with periodic boundaries, meaning that tree crowns protruding the limits of the simulated area on one side reappear on the opposite side.

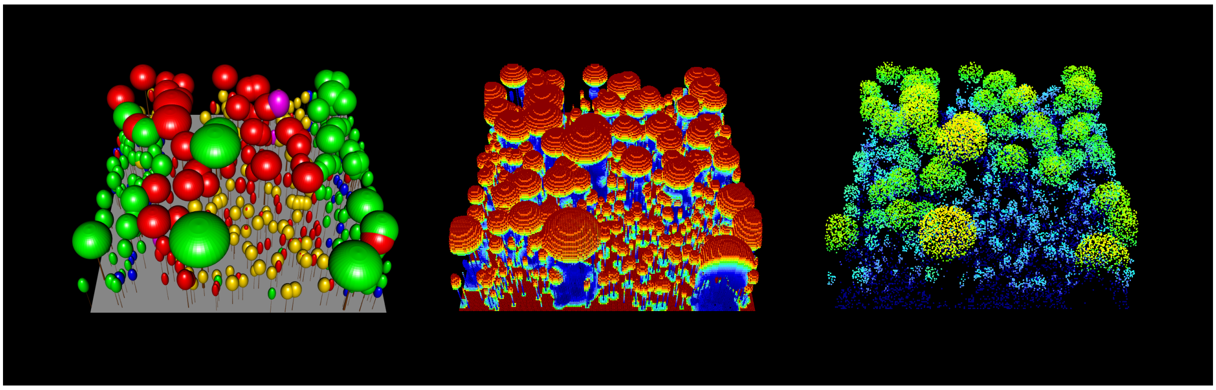

Figure 14: *Schematic visualization of the Lidar model. On the left side a forest stand of 1 ha is shown. In the center you see a voxel representation of the stand with colors indicating Lidar return probability from high (red) to low (blue) for each voxel. On the right side the final simulated point cloud is shown with colors indicating height above ground from 0 m (blue) to 40 m (orange).*

K Input parameter and variables

Table 7: *General input parameter of the simulation.*

Symbol	Description	Unit
A_{area}	simulation area	ha
A_{patch}	patch area	m^2
$n_{patches}$	number of patches per simulation area	
t_y	time step	yr
Δt	time step	yr

Table 8: *Geometrical input parameter.*

Symbol	Description	Unit
h_0, h_1, h_2	coefficients of height-stem diameter-relationship	-
c_{l0}, c_{l1}, c_{l2}	coefficients of crown length-height-relationship	-
c_{d0}, c_{d1}, c_{d2}, c_{d3}	coefficients of crown diameter-stem diameter-relationship	-
ρ	wood density	t_{ODM}/m^3
σ	ratio of total aboveground biomass to stem biomass	-
f	form factor	-
f_0, f_1, f_2	coefficients of form factor-stem diameter-relationship	-
b_0, b_1, b_2	coefficients of biomass-stem diameter-relationship	-
l_0, l_1	LAI-stem diameter-relationship	-
D_{max}	maximum stem diameter	m
H_{max}	maximum height	m
B_{max}	maximum aboveground biomass	t_{ODM}

Table 9: *Recruitment and establishment input parameter.*

Symbol	Description	Unit
N_{seed}	global in-growth rate of seeds	$1/\text{ha yr}$
N_{init}	initial seed number in seed pool	$1/\text{patch}$
D_{rep}	minimum stem diameter of a seed producing mother tree	m
f_{disp}	dispersal kernel	-
$dist$	average dispersal distance	m
σ	ratio of total aboveground biomass to stem biomass	-
I_{seed}	percentage of incoming radiation at floor required for germination	%
M_{pool}	mortality rate of seeds in the seed pool	$1/\text{yr}$
max_{dens}	maximum number of germinating seedlings	$1/\text{patch}$
D_{min}	initial stem diameter of a germinated seedling	m

Table 10: *Mortality input parameter.*

Symbol	Description	Unit
M_B	basic mortality rate	$1/\text{yr}$
m_{d0}, m_{d1}	mortality rate dependent on stem diameter	-
m_{i0}, m_{i1}, m_{i2}	mortality rate dependent on stem diameter increment	-
N_M	min. number of individuals at which stochastic dying is performed	$1/\text{cohort}$
D_M	max. stem diameter below which stochastic dying is performed	m
f_{fall}	probability for a dead tree to fall	-

Table 11: *Light climate and photosynthesis input parameter and variables.*

Symbol	Description	Unit
Δh	width of layers of aboveground vertical space discretization in a patch	m
n_{layer}	number of layer of aboveground vertical space discretization	
I_0	incoming irradiance on top of canopy	$\mu\mathrm{mol_{photon}}/\mathrm{m^2\ s}$
k	light extinction coefficient	-
α	initial slope of light response curve	$\mu\mathrm{mol_{CO_2}}/\mu\mathrm{mol_{photon}}$
p_{max}	maximum leaf gross photosynthetic rate	$\mu\mathrm{mol_{CO_2}}/\mathrm{m^2 s}$
m	transmission coefficient	-
l_{day}	day length	h
φ_{ODM}	conversion factor	$\mathrm{t_{ODM}}/\mu\mathrm{mol_{CO_2}}$

Table 12: *Water module input parameter and variables.*

Symbol	Description	Unit
PR	precipitation	mm/h
K_L	interception constant	mm/h
POR	soil porosity	mm/h
K_s	fully saturated conductivity	mm/h
Θ_{res}	residual soil water content	mm/h
λ	pore size distribution index	-
WUE	water-use-efficiency	t_{ODM}/kg_{H_2O}
PET	potential evapotranspiration	mm/h
Θ_{soil}^{init}	initial soil water content at start of simulation	V%
Θ_{pwp}	permanent wilting point	V%
Θ_{fc}	field capacity	V%
Θ_{msw}	minimum soil water content	V%

Table 13: *Temperature input parameter and variables.*

Symbol	Description	Unit
T	air temperature	$^{\circ}C$
n	number of days per time step Δt	$^{1}/_{\Delta t}$
T_{crit}	critical temperature for bud-burst	$^{\circ}C$
k_0, k_1, k_2	parameter of inhibition factors	-
$T_{CO_2,l}$, $T_{CO_2,h}$	temperature limits of CO_2 assimilation	$^{\circ}C$
T_{hot}, T_{cold}	monthly mean temperature of warmest and coldest month an individual can cope with	$^{\circ}C$
T_{ref}	reference temperature	$^{\circ}C$
Q_{10}	base of Q10 function	-

Table 14: *Respiration input parameter and variables.*

Symbol	Description	Unit
R_g	growth respiration factor	-
$g(D)$	maximum stem diameter increment (growth) function	-
a_0, a_1, a_2, a_3	coefficients of the growth function $g(D)$	-
x_i, $i = 1, ..., 8$	auxillary variables	-
ΔD_{max}	maximum measured stem diameter increment	m/y
$D_{\Delta D_{max}}$	stem diameter at which maximum increment is measured	% of D_{max}
$\Delta D_{D_{min}}$	max. measured stem diameter increment for diameter D_{min}	% of ΔD_{max}
$\Delta D_{D_{max}}$	max. measured stem diameter increment for diameter D_{max}	% of ΔD_{max}
$\check{I_{ind}}$	reference irradiance of parameterization climate	$^{\mu mol_{photon}}/_{m^2 s}$
$\check{\varphi_{act}}$	reference vegetation period of parameterization climate	d
$\check{\varphi_T}$	reference temperature limitation factor of photosynthesis of parameterization climate	-

Table 15: *Lidar input parameter and variables.*

Symbol	Description	Unit
$P_{0,Lid,V}$	Surface return probability for vegetation voxels	-
$k_{Lid,V}$	Lidar extinction coefficient for vegetation voxels	-
$P_{0,Lid,G}$	Surface return probability for ground voxels	-
$k_{Lid,G}$	Lidar extinction coefficient for ground voxels	-
s_{Lid}	Spacing between Lidar pulses	m
t_{Lid}	Time interval between Lidar scans	yr

L State variables

Table 16: *Geometrical state variables.*

Symbol	Description	Unit
D	Stem diameter at breast height	m
H	Height	m
C_D	Crown diameter	m
C_L	Crown length	m
C_A	Crown projection area	m^2
B	Aboveground biomass	t_{ODM}
LAI	Leaf area index	-
ΔB	Biomass increment per time step	t_{ODM}
ΔD	Diameter increment per time step	m

Table 17: *Recruitment and establishment state variables.*

Symbol	Description	Unit
N_{pool}	Seed pool (i.e number of seeds)	$1/\text{patch}$
N_{germ}	Number of successfully germinated seeds	$1/\text{patch}$
N_{est}	Number of successfully established seedlings	$1/\text{patch}$
x_{ind}, y_{ind}	Random position of a mother tree on a patch	-
x_{seed}, y_{seed}	Position of a dispersed seed	-
I_{floor}	Percentage of incoming irradiance at floor	%

Table 18: *Mortality state variables.*

Symbol	Description	Unit
M_D	Mortality rate dependent on stem diameter	$1/\mathrm{yr}$
M_I	Mortality rate dependent on stem diameter increment	$1/\mathrm{yr}$
M	Mortality rate affecting individuals each time step	$1/\mathrm{yr}$
m_{frag}	Factor changing the mortality rate M due to fragmentation	-
CCA_i, $i = 1, ..., \#_{layer}$	Cumulative crown area per height layer	-
l_{min}, l_{max}	Lower and upper height layer covered by the crown of a single individual	-
R_c	Individual crowding reduction factor	-
N_C	Number of individuals dying due to crowding	$1/\mathrm{cohort}$
N_Y	Number of individuals dying due to mortality per time step	$1/\mathrm{cohort}$
N	Number of alive individuals	$1/\mathrm{cohort}$
δ_{rM}	Auxillary variable	-
N_F	Number of individuals affected by a falling tree	-

Table 19: *Light climate and growth state variables.*

Symbol	Description	Unit
$\overline{L_i}$	Individual leaf area contribution to height layer i	m^2
$\widehat{L_i}$	Patch-based leaf area index	-
I_{ind}	Incoming irradiance on top of an individual	$\mu mol_{photon}/m^2\ \mathrm{s}$
I_{leaf}	Incoming irradiance on top of the leaf surface (absorbable radiation)	$\mu mol_{photon}/m^2\ \mathrm{s}$
P_{ind}	Gross photosynthetic rate of an individual	$\mu mol_{CO_2}/\mathrm{yr}$
P_{leaf}	Gross photosynthetic rate of a single leaf	$\mu mol_{CO_2}/m^2\ \mathrm{s}$
GPP	Gross productivity of an individual (possibly reduced)	t_{ODM}/yr
R_m	Maintenance respiration	t_{ODM}/yr
r_m	Maintenance respiration rate	$1/\mathrm{yr}$

Table 20: *Water module state variables.*

Symbol	Description	Unit
Θ_{soil}	Soil water content	mm/h
IN	Interception	mm/h
RO	Run-off	mm/h
$RO_{\rightarrow}$	Surface run-off	mm/h
$RO_{\downarrow}$	Sub-surface run-off	mm/h
TR	Transpiration	mm/h
φ_W	Reduction factor of GPP due to limited soil water	-

Table 21: *Temperature state variables.*

Symbol	Description	Unit
φ_{act}	Length of vegetation period	d
φ_T	Limitation factor of GPP by temperature	-
$\varphi_{T,l}$, $\varphi_{T,h}$	Inhibition factors for low and high temperatures	-
κ_T	Factor affecting maintenance respiration rate r_M by temperature	-

Table 22: Carbon cycle state variables.

Symbol	Description	Unit
S_{dead}	Carbon stock of deadwood	$^{tC}/_{\text{patch}}$
S_{slow}	Carbon amount of slow decomposing soil stock	$^{tC}/_{\text{patch}}$
S_{fast}	Carbon amount of fast decomposing soil stock	$^{tC}/_{\text{patch}}$
S_{mort}	Carbon amount of individuals dying within the current time step	$^{tC}/_{\text{patch}}$
$t_{S_{dead}\to A}$	Transition rate of carbon from deadwood stock S_{dead} to atmosphere A	$^{tC}/_{\text{patch}}$
$t_{S_{slow}\to A}$	Transition rate of carbon from slow decomposing soil stock S_{dead} to atmosphere A	$^{tC}/_{\text{patch}}$
$t_{S_{fast}\to A}$	Transition rate of carbon from fast decomposing soil stock S_{dead} to atmosphere A	$^{tC}/_{\text{patch}}$
$t_{S_{dead}\to}$	Transition rate of carbon from deadwood stock S_{dead} to soil	$^{tC}/_{\text{patch}}$
$t_{S_{dead}\to S_{slow}}$	Transition rate of carbon from deadwood stock S_{dead} to slow decomposing soil stock S_{slow}	$^{tC}/_{\text{patch}}$
$t_{S_{dead}\to S_{fast}}$	Transition rate of carbon from deadwood stock S_{dead} to fast decomposing soil stock S_{fast}	$^{tC}/_{\text{patch}}$
NEE	Net ecosystem exchange	$^{tC}/_{\text{patch}}$
C_{GPP}	Carbon amount of gross productivity per patch	$^{tC}/_{\text{patch}}$
C_R	Carbon amount released by total respiration per patch	$^{tC}/_{\text{patch}}$

Table 23: Disturbances (fire, landslide) state variables.

Symbol	Description	Unit
N_D	Number of individuals dying due to disturbances	$^{1}/_{\text{cohort}}$
P_{F_1}, P_{F_2}, P_{F_3}, P_{F_4}	Burning probabilities for the 4 fire tolerance levels	-

Table 24: *Lidar state variables.*

Symbol	Description	Unit
d_{Lid}	Number of vegetation voxels above a focal voxel, corresponds to distance that the laser beam traveled within tree canopy space	m
P_{Lid}	Probability of a voxel to contain a Lidar return	-

M Abbreviations

Symbol	Description
ODM	Organic dry matter
CO_2	Carbon dioxide
C	Carbon
H_2O	Water
sin	Sinus function
cos	Cosinus function
$\lfloor\rfloor$	Round down
e	Exponential function
ln	Logarithm function
cf.	see
e.g.	exempli gratia (for example)
i.e.	id est (that is)
Fig.	Figure
Tab.	Table

References

Botta, A., Viovy, N., Ciais, P., Friedlingstein, P., Monfray, P., 2000. A global prognostic scheme of leaf onset using satellite data. Global Change Biology 6, 709–725.

Busing, R.T., Solomon, A.M., 2006. Modeling the effects of fire frequency and severity on forests in the northwestern United States. Scientific Investigations Report 2006-5061, US Geological Survey.

Dislich, C., Günter, S.and Homeier, J., Schröder, B., Huth, A., 2009. Simulating forest dynamics of a tropical montane forest in south ecuador. Erdkunde 63, 347–364.

Dislich, C., Huth, A., 2012. Modelling the impact of shallow landslides on forest structure in tropical montane forests. Ecological Modelling 239, 40–53.

Fischer, R., 2010. Modellierung des Wachstums von Regenwäldern. Untersuchung der Auswirkungen von Trockenstress und Holznutzung auf den tropischen Regenwald am Beispiel des RNI Betampona (Madagaskar). Master's thesis. HTWK Leipzig.

Gardner, R.H., Romme, W.H., Turner, M.G., 1999. Predicting forest fire effects at landscape scales, in: Mladenoff, D.J., Baker, W.L. (Eds.), Spatial Modeling of Forest Landscape Change: Approaches and Applications., Cambridge University Press, Cambridge. pp. 163–185.

Granier, A., BrÃ©da, N., Biron, P., Villette, S., 1999. A lumped water balance model to evaluate duration and intensity of drought constraints in forest stands. Ecological Modelling 116, 269–283.

Green, D.G., 1989. Simulated effects of fire, dispersal and spatial pattern on competition within forest mosaics. Vegetatio 82, 139–153.

Gutiérrez, A.G., Huth, A., 2012. Successional stages of primary temperate rainforests of chiloé island, chile. Perspectives in Plant Ecology, Evolution and Systematics 14, 243–256.

Haxeltine, A., Prentice, C.I., 1996. A general model for the light-use efficiency of primary production. functional ecology 10, 551–561.

Huth, A., Ditzer, T., 2001. Long-term impacts of logging in a tropical rain forest - a simulation study. Forest Ecology and Management 142, 33 – 51.

Huth, A., Drechsler, M., Koehler, P., 2005. Using multicriteria decision analysis and a forest growth model to assess impacts of tree harvesting in dipterocarp lowland rain forests. Forest Ecology and Management 207, 215 – 232. Decision Support in Multi

Purpose Forestry Decision Support in Multi Purpose Forestry Selected papers from the symposium on Development and Application of Decision Support Tools in Multiple Purpose Forest Management.

Keane, R.E., Cary, G.J., Davies, I.D., Flannigan, M.D., Gardner, R.H., Lavorel, S., Lenihan, J.M., Li, C., Rupp, T.S., 2004. A classification of landscape fire succession models: spatial simulations of fire and vegetation dynamics. Ecological Modelling 179, 3–27.

Kumagai, T., Katul, G.G., Saitoh, T.M., Sato, Y., Manfroi, O.J., Morooka, T., Ichie, T., Kuraji, K., Suzuki, M., Porporato, A., 2004. Water cycling in a bornean tropical rain forest under current and projected precipitation scenarios. Water Resour. Res. 40, W01104–.

Lambers, H., Chapin III, F., Pons, T., 2008. Plant physiological ecology. Springer.

Larcher, W., 2001. Ökophysiologie der Pflanzen. Leben, Leistung und Stressbewältigung der Pflanzen in ihrer Umwelt. UTB für Wissenschaft, Verlag Eugen Ulmer Stuttgart.

Liang, X., Lettennmaier, D., Wood, E., Burges, S.J., 1994. A simple hydrologically based model of land surface water and energy fluxes for general circulation models. Journal of Geophysical Research 99, 14415–14428.

Monsi, M., Saeki, T., 1953. Uber den lichtfaktor in den pflanzengesellschaften und seine bedeutung fur die stoffproduktion. Jpn. J. Bot 17, 22–52.

Pfeiffer, M., Spessa, A., Kaplan, J.O., 2013. A model for global biomass burning in preindustrial time: Lpj-lmfire (v1.0). Geoscientific Model Development 6, 643–685.

Prentice, C.I., Sykes, M.T., Cramer, W., 1993. A simulation model for the transient effects of climate change on forest landscapes. Ecological Modelling 65, 51–70.

Sato, H., Itoh, A., Kohyama, T., 2007. Seib-dgvm: A new dynamic global vegetation model using a spatially explicit individual-based approach. Ecological Modelling 200, 279–307.

Thonicke, K., Venevsky, S., Sitch, S., Cramer, W., 2001. The role of fire disturbance for global vegetation dynamics: coupling fire into a dynamic global vegetation model. Global Ecology and Biogeography 10, 661–677.

Thornley, J.H.M., Johnson, I.R., 1990. Plant and crop modelling: a mathematical approach to plant and crop physiology. Oxford University Press.

Wilcke, W., Valladarez, H., Stoyan, R., Yasin, S., Valarezo, C., Zech, W., 2003. Soil properties on a chronosequence of landslides in montane rain forest, ecuador. CATENA 53, 79–95.